

Proof-of-work consensus by quantum sampling

Deepesh Singh,^{1,*} Boxiang Fu,^{2,†} Gopikrishnan Muraleedharan,^{3,‡} Chen-Mou Cheng,^{4,§} Nicolas Roussy Newton,^{4,¶} Peter P. Rohde,^{5,6,**} and Gavin K. Brennen^{3,††}

¹*Centre for Quantum Computation & Communications Technology,
School of Mathematics & Physics, The University of Queensland, St Lucia QLD 4072, Australia*

²*School of Physics, University of Melbourne, Melbourne, VIC 3010, Australia*

³*Center for Engineered Quantum Systems, School of Mathematical
and Physical Sciences, Macquarie University, NSW 2109, Australia*

⁴*BTQ Technologies, 16-104 555 Burrard Street, Vancouver BC, V7X 1M8 Canada*

⁵*Centre for Quantum Software & Information (UTS:QSI), University of Technology Sydney*

⁶*Hearne Institute for Theoretical Physics, Department of Physics & Astronomy,
Louisiana State University, Baton Rouge LA, United States*

Since its advent in 2011, boson-sampling has been a preferred candidate for demonstrating quantum advantage because of its simplicity and near-term requirements compared to other quantum algorithms. We propose to use a variant, called coarse-grained boson-sampling (CGBS), as a quantum Proof-of-Work (PoW) scheme for blockchain consensus. The users perform boson-sampling using input states that depend on the current block information, and commit their samples to the network. Afterward, CGBS strategies are determined which can be used to both validate samples and to reward successful miners. By combining rewards to miners committing honest samples together with penalties to miners committing dishonest samples, a Nash equilibrium is found that incentivizes honest nodes. The scheme works for both Fock state boson sampling and Gaussian boson sampling and provides dramatic speedup and energy savings relative to computation by classical hardware.

I. INTRODUCTION

Blockchain technology relies on the ability of a network of non-cooperating participants to reach consensus on validating and verifying a new set of block-bundled transactions, in a setting without centralized authority. A consensus algorithm is a procedure through which all the peers of the blockchain network reach a common agreement about the present state of the distributed ledger. One of the best tested consensus algorithms which has demonstrated robustness and security is Proof-of-Work (PoW) [1]. PoW relies on validating a proposed block of new transactions to be added to the blockchain by selecting and rewarding a successful “miner” who is the first to solve a computational puzzle. This puzzle involves a one-way function, i.e. a function that is easy to compute, and hence easy to verify, but hard to invert. Traditionally the chosen function is the inverse hashing problem, which by its structure makes the parameters of the problem dependent on the current block information, thus making pre-computation infeasible. Additionally the problem is progress-free, meaning the probability of successfully mining a block at any given instant is independent of prior mining attempts. This means a miner’s success probability essentially grows linearly with

the time spent, or equivalently work expended, solving the problem. The later feature ensures that the mining advantage is proportionate to a miner’s hashing power.

There are, however, two issues that threaten to compromise continued usage of PoW consensus in a scalable manner. The first is energy consumption. Problems like inverse hashing admit fast processing, now at speeds of tens of THash/s, by application specific integrated circuits (ASICs). Unfortunately, the tremendous speed of these devices come at the cost of large power consumption, and as the hashing power of the network grows so grows the energy cost per transaction. The reason is for asset-based cryptocurrencies like Bitcoin, as the overall network hashing power grows, the difficulty of the one way function is increased to maintain a constant transaction speed. Since new Bitcoin are introduced through the mining process, a constant transaction speed is desirable to maintain stability and to avoid inflationary pressures. As of May, 2023, a single Bitcoin transaction had the equivalent energy consumption of an average U.S. household over 19.1 days (Digiconomist).

The energy consumption of PoW blockchains has several negative consequences. It contributes to climate change by generating large amounts of carbon emissions when the source of energy is non-renewable. Additionally, it creates a significant financial burden for miners, who must pay for the electricity and equipment required to mine blocks effectively. This can lead to the centralization of mining power in the hands of a few large mining pools, potentially compromising the network’s security and decentralization.

Moreover, the energy consumption of PoW blockchains can be seen as wasteful and unnecessary, given that there

* deepesh.singh@uq.edu.au

† boxiangf@student.unimelb.edu.au

‡ gopikrishnan.muraleedharan@mq.edu.au

§ cheng@btq.li

¶ nic@btq.li

** dr.rohde@gmail.com

†† gavin.brennen@mq.edu.au

are alternative consensus mechanisms, such as Proof-of-Stake (PoS), that require significantly less energy to operate. However, PoS has some other liabilities such as the plutocratic feature of mining power being dependent on the number of coins held by a miner, and vulnerability to other attack vectors like “long range” and “nothing at stake” attacks. As a result, there have been growing calls for the development of more sustainable and environmentally friendly blockchain technologies.

The second issue is that PoW assumes only classical computers are available as mining resources. Quantum computing technology, while only at the prototype stage now, is rapidly developing. Quantum computers running Grover’s search algorithm [2], can achieve a quadratic speedup in solving unstructured problems like inverting one-way functions. This means if they were integrated into PoW, the progress-free condition would no longer apply and the probability of solving the problem grows super-linearly with computational time spent¹. An adversarial network of future quantum computers performing PoW consensus will have radically different behaviour, such as probabilistic computing strategies and large fluctuations in the time to solve [3]. Workarounds can be found, such as using random beacons which interrupt the search progress of quantum computers by periodically announcing new puzzles to be solved, as suggested in Ref. [4]. However, as quantum computers speedup and are parallelized, the frequency of beacons will need to increase to avoid distortions in the consensus dynamics. A future-proofed consensus algorithm should take quantum processing into account as a core resource.

As mentioned above, for unstructured search problems Grover’s algorithm provides a quadratic advantage over the best-known classical algorithms. This gap between the classical and quantum algorithms’ runtimes can be increased in more specific tasks like prime factorisation and discrete logarithm to provide exponential speedups [5, 6]. The accomplishment of these exponential speedups however requires large-scale fault-tolerant quantum computers that will not be available for some time. Moreover, as discussed, such algorithms would violate the progress-free condition. This motivates the search for practical applications of the advantages provided by noisy intermediate-scale quantum (NISQ) devices [7].

We propose a new PoW consensus protocol based on boson-sampling. Boson-sampling was originally developed to demonstrate *quantum supremacy*, owing to its reduced resource requirements compared to the other quantum algorithms [8]. Boson-samplers are specialized photonic devices that are restricted in the sense that they are neither capable of universal quantum computing nor error correctable, through proposals have been made to find

practical applications in chemistry, many-body physics, and computer science [7]. We formulate a practical application of a boson-sampling variant called coarse-grained boson-sampling (CGBS) [9, 10]. This scheme involves the equal size grouping of the output statistics of a boson-sampler into a fixed number of bins according to some given binning tactic.

The advantage provided by binning the output probability distribution is the polynomial number of samples required to verify a fundamental property of the distribution as opposed to the exponential samples required when no binning is performed. While boson-samplers are not arbitrarily scalable owing to lack of error correction, we argue nonetheless the speedup provided is dramatic enough to warrant their use for PoW consensus.

Photonic based blockchain has been investigated before. Optical PoW [11] uses HeavyHash, a slight modification of the Bitcoin protocol, where a photonic mesh-based matrix-vector product is inserted in the middle of mining. This has already been integrated into the cryptocurrencies optical Bitcoin and Kaspas. Recently, a more time and energy efficient variant named LightHash has been tested on networks of up to 4 photons [12]. Both of these protocols use passive linear optics networks acting upon coherent state inputs which implement matrix multiplication on the vector of coherent amplitudes. It is conjectured that the photonic implementation of this matrix multiplication can achieve an order of magnitude speedup over traditional CPU hardware. They exploit the *classical* speedup associated with photonic implementation of this operation and do not exploit any quantum advantage. While that method uses a multi-mode interferometer similar to what we describe in this work, it does not use intrinsically quantum states of light and in fact is a different form of classical computing using light. In contrast, our boson sampling method uses quantum resources with processes that become exponentially harder, in the number of photons, to simulate with classical hardware whether photonic or not.

II. BACKGROUND

A. Blockchains

A blockchain is a decentralized and distributed ledger that stores transactions in a secure and transparent manner. The ledger consists of a chain of fixed-length blocks, each of which is verified by every node in the network. The network is decentralized, meaning no central authority exerts control, relying on a network of nodes to maintain its integrity. Each block is then added to the blockchain once a decentralized consensus is reached. The whole process is illustrated in Fig. 1 and can be described as follows:

1. Transaction Verification: Transactions are sent to the network. Before a transaction can be included

¹ Specifically the probability to solve in time t grows like $p(t) = \sin^2(ct)$, where $c = O(\sqrt{D/H})$, H is the size of the search domain for the one-way function, and D is the number of satisfying arguments.

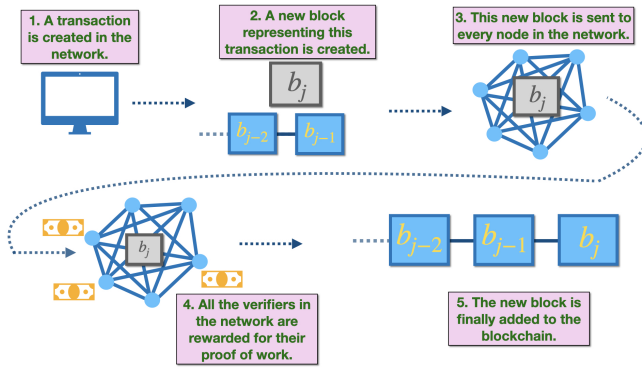


Figure 1. Blockchain architecture and the addition of new blocks.

in a block, it must be validated by nodes on the network. Each node checks that the transaction is legitimate and that the sender has sufficient funds to complete the transaction.

2. **Block Creation:** Once a group of transactions is verified, they are bundled together into a block. The block contains a header, which includes the previous block's hash, a timestamp, and a *nonce* (a random number).
3. **Proof-of-Work:** To mine the block, miners compete to solve a complex mathematical puzzle, known as Proof-of-work (PoW). The first miner to solve the puzzle broadcasts their solution to the network, and the other nodes verify the solution. If the solution is correct, the miner is rewarded with newly minted cryptocurrency, and the block is added to the blockchain.
4. **Consensus Mechanism:** To maintain the integrity of the blockchain, the network must reach a consensus on the state of the ledger. In a decentralized blockchain network, this is achieved through a consensus mechanism, such as PoW or Proof-of-Stake (PoS). PoW requires miners to compete to solve a mathematical puzzle, while PoS relies on validators who hold a stake in the network to verify transactions.
5. **Block Confirmation:** Once a block is added to the blockchain, it cannot be altered or deleted. Other nodes on the network can confirm the block by verifying the hash of the previous block, ensuring that the chain is continuous and secure.

1. One-way functions

Blockchain technology relies heavily on one-way functions as a critical component of its security infrastructure. One-way functions are mathematical functions that are

easy to compute in one direction but difficult to reverse. The public-key cryptography used in blockchains today relies on pairs of related keys (public and private) generated by one-way functions. While it is easy to compute a public key from a private key, the reverse operation is computationally intractable. This makes private keys extremely difficult to guess or brute-force, thus ensuring the security of blockchain networks. Hash functions are another example of one-way functions with widespread cryptographic utility.

More precisely, one-way functions are easy to compute for all inputs in their domain, but hard to invert given the image of any unknown input. That is, given a function,

$$f(x) = y, \quad (2.1)$$

y is easy to compute for all inputs x , however computing x for a given y is hard. Computationally speaking, the notions of 'easy' and 'hard' refer to polynomial-time and super-polynomial-time algorithms respectively in input size. Therefore, in general, the inversion of one-way functions resides within the computational complexity class **NP** since the verification of any pre-image is possible in polynomial time, unlike its explicit computation.

These one-way functions are of importance in various applications including cryptography and authentication protocols. Their existence is still an open conjecture and if proven, has serious computational complexity theoretic implications, including that of $\mathbf{P} \neq \mathbf{NP}$, hence the interest in their discovery. Nevertheless, there are many favourable candidates for one-way functions, i.e. functions for which no polynomial-time inversion algorithms are known. It is important to note that no rigorous proof of the non-existence of these inversion algorithms exists.

2. Hash functions

A general hash function is a one-way function that satisfies three main properties:

- Its input can be of any size.
- Its output is always of a fixed size.
- It should be easy to compute.

A cryptographic hash function has several additional requirements [13]:

- **Collision-free:** A hash function H is said to be collision resistant if it is infeasible to find two values, x and y , where $H(x) = H(y)$ and $x \neq y$.
- **Hiding:** A hash function H is hiding if it is infeasible to find x , given $H(r||x)$, where r is a secret value that is chosen from a probability distribution with high min-entropy.
- **Puzzle friendliness:** A hash function H is said to be puzzle-friendly if for every possible n -bit output

value y , if k is chosen from a distribution with high min-entropy, then it is infeasible to find x such that $H(k||x) = y$ in time significantly less than 2^n .

In some existing classical blockchain implementations, notably Bitcoin, partial inverse hashing is employed for the purposes of PoW. Here the miners compete to find bitstrings that hash to an output string with some number of leading zeros. The number of required leading zeroes translates to the difficulty of solving this problem. Since hash functions are highly unstructured, the best classical approach to finding such solutions is using brute force to hash random input strings until by chance a satisfying output is found. Once found, it is trivial for other nodes to verify the solution by simply hashing it.

State-binned boson-sampling (see Sec. II B 3) was motivated as an attempt to construct a hash function – a one-way decision function – from the boson-sampling problem [10]. Note that such a definition for a hash function differs from conventional hash functions, as it is not in **NP**, since a classical verifier cannot efficiently verify the output to the hash given the input state.

Here we do not employ this full hash function construction directly, but taking inspiration from it employ the peak bin probability as a signature of the operation of a boson-sampling device. While a classical verifier is unable to verify the peak bin probability given the input state, independent quantum boson samplers will converge upon the same estimated peak bin probability. This is sufficient for the purposes of consensus, where samples provided by different parties can be cross-checked for convergence upon the same estimate, despite it not being classically efficient to determine whether that estimate is correct.

3. Hash pointers and data structures

A regular pointer stores the memory address of data, making it easy to access. On the other hand, a hash pointer is a pointer that stores the cryptographic hash of the data along with its memory address. Thus, a hash pointer points to data while enabling verification ([weblink](#)).

Moreover, a *linked list* is a linear collection of data elements where each element contains both data and a pointer to the previous element. The order of a linked list is not given by their physical placement in memory ([wiki](#)). A blockchain then is a linked list with a hash pointer to the previous element, which assists in the verification of the previous element's data.

B. Boson-sampling

Boson-sampling [8, 14] is the problem of sampling multi-mode photo-statistics at the output of a randomised optical interferometer. This problem constitutes

a noisy intermediate scale quantum (NISQ) [15] protocol, naturally suited to photonic implementation. Like other NISQ protocols, boson sampling is not believed to be universal for quantum computation, nor does it rely on error correction, thereby limiting scalability. Nonetheless, it has been shown² to be a classically inefficient yet quantum mechanically efficient protocol, making it suitable for demonstrating *quantum supremacy*, which is now believed to have been achieved [16, 17].

Unlike *decision problems*, which provide a definitive answer to a question, boson-sampling is a *sampling problem* where the goal is to take measurement samples from the large superposition state exiting the device.

Since boson-sampling is not an **NP** problem [18], the full problem cannot be efficiently verified by classical or quantum computers. Indeed, even another identical boson sampler cannot be used for verification since results are probabilistic and in general unique, ruling out a direct comparison of results as a means of verification. Nonetheless, restricted versions of the problem such as coarse-grained boson sampling, described below, can be used for verification.

1. Fundamentals

The general setup for the boson sampling problem is illustrated in Fig. 2. We take M optical modes of which N are initialised with the single-photon state and $M - N$ with the vacuum state at the input,

$$\begin{aligned} |S\rangle &= |1\rangle^{\otimes N} \otimes |0\rangle^{\otimes M-N} \\ &= \hat{a}_1^\dagger \dots \hat{a}_N^\dagger |0\rangle^{\otimes M}, \end{aligned} \quad (2.2)$$

where \hat{a}_i^\dagger is the photonic creation operator on the i th mode. Choosing $M \geq O(N^2)$ ensures that with a high likelihood the output state remains in the anti-bunched regime whereby modes are occupied by at most one photon. Hence, such samples may be represented as m -bit binary strings.

The input state is evolved via passive linear optics comprising beamsplitters and phase-shifters, implementing the Heisenberg transformation on the photonic creation operators,

$$\hat{U} \hat{a}_i^\dagger \hat{U}^\dagger \rightarrow \sum_{j=1}^M U_{i,j} \hat{a}_j^\dagger, \quad (2.3)$$

where U is the $M \times M$ unitary matrix representing the multi-mode linear optics transformation³. That is, each

² Under reasonable complexity-theoretic assumptions.

³ To be distinguished from the operator (with a hat) \hat{U} that is an exponential of a bilinear form of creation and annihilation operators.

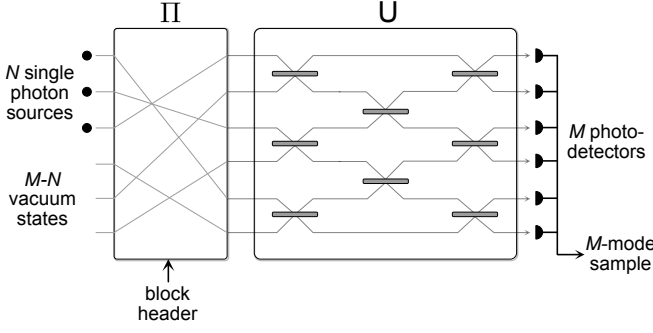


Figure 2. Illustration of the use of a boson-sampling device for blockchain consensus. Initially, N photons are incident in the first N modes, with the remaining $M - N$ modes in the vacuum state. The modes then undergo a permutation Π dependent on the block header information, which in practice would be accomplished by simply permuting the locations of the single-photon inputs. The photons then pass through an interferometer circuit of depth M described by unitary U . Finally, the photons are detected at the M output ports providing a measurement record of the sample.

input photonic creation operator is mapped to a linear combination of creation operators over the output modes.

The linear optics transformation U is chosen uniformly at random from the Haar measure, essential to the underlying theoretical complexity proof. It was shown by [19] that any $M \times M$ linear optics transformation of the form shown in Eq. 2.3 can be decomposed into a network of at most $O(M^2)$ beamsplitters and phase-shifters, ensuring that efficient physical implementation is always possible. As presented in Fig. 2, the number of detectors equals the number of modes M . In practice, the number of detectors can be reduced by exploiting multiplexing in other degrees of freedom, such as the temporal degree of freedom. For example, in the architecture presented in Ref. [20], where modes are encoded temporally, a single time-resolved detector is sufficient for detecting and distinguishing between all modes.

The output state takes the general form,

$$|\psi\rangle_{\text{out}} = \left[\prod_{i=1}^N \sum_{j=1}^M U_{i,j} \hat{a}_j^\dagger \right] |0\rangle^{\otimes M} \quad (2.4)$$

$$= \sum_{k=1}^{|Y|} \alpha_k |Y_k\rangle,$$

where $|Y_k\rangle = |y_1^{(k)}, \dots, y_M^{(k)}\rangle$ denotes the occupation number representation of the k th term in the superposition with $y_i^{(k)}$ photons in the i th mode, and α_k is the respective quantum amplitude, where for normalisation,

$$\sum_{k=1}^{|Y|} |\alpha_k|^2 = 1. \quad (2.5)$$

The number of terms in the superposition is given by,

$$|Y| = \binom{M + N - 1}{N}, \quad (2.6)$$

which grows super-exponentially with M in the $M \geq O(N^2)$ regime. Since we are restricted to measuring a number of samples polynomial in N from an exponentially large sample space, we are effectively guaranteed to never measure the same output configuration multiple times. Hence, the boson-sampling problem is *not* to reconstruct the full photon-number distribution given in Eq. 2.4, but rather to incompletely sample from it.

In the lossless case, the total photon number is conserved. Hence,

$$\sum_{i=1}^M x_i = \sum_{i=1}^M y_i^{(k)} = N \quad \forall X, Y, k, \quad (2.7)$$

where $|X\rangle = |x_1, \dots, x_M\rangle$ represents the occupation number representation of the input state.

The amplitudes in the output superposition state are given by,

$$\alpha_k = \langle Y_k | \hat{U} | X \rangle = \frac{\text{Per}(U_{X,Y_k})}{\sqrt{\prod_{i=1}^M x_i! y_i^{(k)}!}}, \quad (2.8)$$

where $\text{Per}(\cdot)$ denotes the matrix permanent, and $U_{X,Y}$ is an $N \times N$ sub-matrix of U composed by taking x_i copies of each row and $y_i^{(k)}$ copies of each column of U . The permanent arises from the combinatorics associated with the multinomial expansion of Eq. 2.4, which effectively sums the amplitudes over all possible paths input photons X may take to arrive at a given output configuration Y_k .

The probability of measuring a given output configuration Y_k is simply,

$$\Pr(Y_k) = |\alpha_k|^2. \quad (2.9)$$

In lossy systems with uniform per-photon loss η , all probabilities acquire an additional factor of η^N upon post-selecting on a total of N measured photons,

$$\Pr(Y_k) = \eta^N |\alpha_k|^2. \quad (2.10)$$

The overall success probability of the device is similarly,

$$\Pr_{\text{success}} = \eta^N. \quad (2.11)$$

Calculating matrix permanents is $\#\mathbf{P}$ -hard in general, a complexity class even harder than \mathbf{NP} -hard⁴, from which the classical hardness of this sampling problem

⁴ $\#\mathbf{P}$ is the class of counting problem equivalents of \mathbf{NP} decision problems. While the class of \mathbf{NP} problems can be defined as finding a satisfying input to a boolean circuit yielding a given output, $\#\mathbf{P}$ enumerates *all* satisfying inputs.

arises. It should however be noted that boson-sampling does not let us efficiently *calculate* matrix permanents as this would require knowing individual amplitudes α_k . The α_k amplitudes cannot be efficiently measured since we are only able to sample a polynomial subset of an exponentially large sample space, effectively imposing binary accuracy as any output configuration is unlikely to be measured more than once.

The class of sampling problems that can be efficiently solved on a universal quantum computer is defined as **SampBQP**. Boson sampling is not universal and defined by its own complexity class **BosonSampP**, which is (likely strictly) contained in **SampBQP**. Thus, **BosonSampP** \subseteq **SampBQP**. Boson sampling is also not believed to be universal for classical sampling problems, **SampP**, which are believed to be incomparable classes.

The complexity proof of boson-sampling presented in [8] is not a direct proof per se, but rather a proof that if boson-sampling were efficiently classically simulatable this would have complexity theoretic implications considered highly unlikely, although not proven. This effectively reduces the argument to one that has been well-studied. Specifically, it was shown using the results in [21] and other arguments that efficient classical simulation of the boson-sampling problem, including approximate boson-sampling, would imply a collapse of the polynomial hierarchy, **PH**, to the third level. It is important to note that, for the case of approximate boson-sampling problem, there are additional conjectures that are assumed to be true for the complexity results [8]. The polynomial hierarchy is an oracle-based generalisation of the complexity classes **P** and **NP**, where an *oracle* is a theoretical device that can be queried to spontaneously provide solutions to problems in a given complexity class. **P** and **NP** are contained in the zeroth and first levels of **PH** respectively. An **NP** device with access to an **NP** oracle is denoted **NP^{NP}**, which is contained in the second level of **PH**. This oracle-based definition generalises to form the full polynomial hierarchy. In the same way that it is strongly believed, but not proven, that **P** \neq **NP**, it is firmly believed, but not proven, that all levels of **PH** are distinct. The boson-sampling complexity proof shows that if boson-sampling could be efficiently classically simulated, this would imply a *collapse* in **PH**, whereby levels are not distinct. Thus, if it is the case the levels of **PH** are distinct — strongly believed to be the case — boson-sampling is a classically hard problem.

2. Mode-binned boson-sampling

Consider an N -photon, M -mode boson-sampling experiment where the output modes are arranged in $d^{(\text{mb})}$ bins labelled $\text{bin}_1^{(\text{mb})}, \text{bin}_2^{(\text{mb})}, \dots, \text{bin}_{d^{(\text{mb})}}^{(\text{mb})}$. Given a linear optical unitary \hat{U} on M modes, let $P(\mathbf{n})$ be the probability of measuring the multi-photon binned number output described by the output vector $\mathbf{n} = (n_1, n_2, \dots, n_{d^{(\text{mb})}})$,

with n_i photons in bin_i . It was shown in [22] that this distribution can be expressed as the discrete Fourier transform over the characteristic function,

$$P^{(\text{mb})}(\mathbf{n}) = \frac{1}{(N+1)^{d^{(\text{mb})}}} \sum_{\mathbf{c} \in \mathbb{Z}_{N+1}^{d^{(\text{mb})}}} \chi\left(\frac{2\pi\mathbf{c}}{N+1}\right) e^{-i\frac{2\pi\mathbf{c} \cdot \mathbf{n}}{N+1}}, \quad (2.12)$$

where,

$$\chi(\mathbf{s}) = \langle \Psi_{\text{in}} | \hat{U}^\dagger e^{i2\pi\mathbf{s} \cdot \hat{\mathbf{N}}_{d^{(\text{mb})}}} \hat{U} | \Psi_{\text{in}} \rangle, \quad (2.13)$$

and the vector of binned number operators is,

$$\hat{\mathbf{N}}_{d^{(\text{mb})}} = \left(\sum_{j_1 \in \text{bin}_1^{(\text{mb})}} \hat{n}_{j_1}, \dots, \sum_{j_{d^{(\text{mb})}} \in \text{bin}_{d^{(\text{mb})}}^{(\text{mb})}} \hat{n}_{j_{d^{(\text{mb})}}} \right). \quad (2.14)$$

The characteristic function can be computed directly as a matrix permanent,

$$\chi(\mathbf{s}) = \text{Per}(V_N(\mathbf{s})), \quad (2.15)$$

with,

$$V(\mathbf{s}) = U^\dagger D(\mathbf{s}) U, \quad (2.16)$$

where the diagonal matrix $D(\mathbf{s}) = \prod_{j=1}^{d^{(\text{mb})}} D^{(j)}(s_j)$ and

$$[D^{(j)}(s_j)]_{u,v} = \begin{cases} 1 & \text{if } u = v \text{ and } u \notin \text{bin}_j^{(\text{mb})} \\ e^{is_j} & \text{if } u = v \text{ and } u \in \text{bin}_j^{(\text{mb})} \\ 0 & \text{if } u \neq v \end{cases}. \quad (2.17)$$

Here $V_N(\mathbf{s})$ means taking the $N \times N$ matrix formed from the N rows and N columns of the $M \times M$ matrix V according to the mode location of single-photon inputs in the input vector $|\Psi_{\text{in}}\rangle$.

By Eq. 2.12, the mode-binned probability distribution can be computed by evaluating $(N+1)^{d^{(\text{mb})}}$ permanents. To exactly compute the permanent of an $N \times N$ matrix requires $O(N2^N)$ elementary operations using Ryser's algorithm, but if we only demand a polynomial additive approximation then a cheaper computational method is available. We can use the Gurvitz approximation which allows for classical estimation of the permanent of a complex $N \times N$ matrix to within additive error δ in $O(N^2/\delta^2)$ operations. The algorithm works by sampling random binary vectors and computing a Glynn estimator (Appendix A). The number of random samples m needed to approximate $\chi(\mathbf{s})$ to within δ with probability at least p is,

$$m = \frac{2}{\delta^2} \ln(2/(1-p)), \quad (2.18)$$

and each Glynn estimator can be computed in N^2 elementary steps. We use now the definition of total variation distance between two distributions with support in

some domain D as,

$$\mathcal{D}^{(\text{tv})}(P, Q) \equiv \frac{1}{2} \sum_{\mathbf{x} \in D} |P(\mathbf{x}) - Q(\mathbf{x})|. \quad (2.19)$$

It is shown in Ref. [22] that by choosing

$$\delta \leq \frac{\beta}{(N+1)^{d^{(\text{mb})}/2}}, \quad (2.20)$$

an estimate $\widehat{P^{(\text{mb})}}(\mathbf{n})$ of the mode-binned distribution can be obtained such that $\mathcal{D}^{(\text{tv})}(\widehat{P^{(\text{mb})}}, P^{(\text{mb})}) \leq \beta$. The number of elementary operations to compute this estimate is⁵,

$$\frac{2 \ln(2/(1-p)) N^{2d^{(\text{mb})}+2} \log(N)}{\beta^2}. \quad (2.21)$$

For a fixed $d^{(\text{mb})}$, this provides a classical polynomial time in N approximation to the mode-binned distribution. Regarding the number of quantum samples needed, it has been shown [23] that if one has the means to draw samples from a distribution Q , the number of samples N_{tot} needed to distinguish Q from another distribution P is,

$$\frac{c\sqrt{|D|}}{\mathcal{D}^{(\text{tv})}(Q, P)^2}. \quad (2.22)$$

Here, choosing the constant $c = 2^{16}$ assures that the test succeeds with probability at least 3/4. For the mode-binned boson-sampling distribution, we can choose Q to be the distribution from which nodes are sampling from $P_{\text{BS}}^{(\text{mb})}(\mathbf{n})$, and P to be the estimate of the true distribution $\widehat{P^{(\text{mb})}}(\mathbf{n})$. The dimension $|D|$ will be the total number of ways N photons can be put in $d^{(\text{mb})}$ bins. This is given by,

$$|D| = \binom{N + d^{(\text{mb})} - 1}{N}. \quad (2.23)$$

We want to guarantee that the following cases are rejected,

$$\mathcal{D}^{(\text{tv})}(P^{(\text{mb})}(\mathbf{n}), P_{\text{BS}}^{(\text{mb})}(\mathbf{n})) \geq \beta. \quad (2.24)$$

Since the total variation distance is a distance metric, we can write,

$$\begin{aligned} & \mathcal{D}^{(\text{tv})}(P^{(\text{mb})}(\mathbf{n}), P_{\text{BS}}^{(\text{mb})}(\mathbf{n})) \\ & \geq \mathcal{D}^{(\text{tv})}(P_{\text{BS}}^{(\text{mb})}(\mathbf{n}), \widehat{P^{(\text{mb})}}(\mathbf{n})) - \mathcal{D}^{(\text{tv})}(P^{(\text{mb})}(\mathbf{n}), \widehat{P^{(\text{mb})}}(\mathbf{n})) \\ & \geq \mathcal{D}^{(\text{tv})}(P_{\text{BS}}^{(\text{mb})}(\mathbf{n}), \widehat{P^{(\text{mb})}}(\mathbf{n})) - \beta, \end{aligned} \quad (2.25)$$

where we have used the fact that $\mathcal{D}^{(\text{tv})}(P^{(\text{mb})}, \widehat{P^{(\text{mb})}}(\mathbf{n})) \leq \beta$. So in order to reject cases in Eq: 2.24, the following has to be true,

$$\mathcal{D}^{(\text{tv})}(\widehat{P^{(\text{mb})}}(\mathbf{n}), P_{\text{BS}}^{(\text{mb})}(\mathbf{n})) \geq 2\beta \quad (2.26)$$

The number of samples needed to distinguish the estimate $P^{(\text{mb})}$ from P_{BS} that is more than 2β in total variation distance away is,

$$N_{\text{tot}}^{(\text{mb})} = 2^{14} \frac{\sqrt{\binom{N+d^{(\text{mb})}-1}{N}}}{\beta^2}. \quad (2.27)$$

3. State-binned boson-sampling

An alternative to the above procedure where bins are defined by sets of output modes is to bin according to sets of multimode Fock states. For an N -photon input state in an M -mode unitary U , the number of possible output configurations is given by $|Y|$ as defined in Eq. 2.6. State-binned boson sampling then concerns the binning of this $|Y|$ dimensional Hilbert space into $d^{(\text{sb})}$ bins.

For a given boson-sampling experiment, the output samples are essentially the $|Y_k\rangle$ configuration vectors as defined in Eq. 2.4, where $1 \leq k \leq \binom{N+M-1}{N}$. However, the state-binned samples into $d^{(\text{sb})}$ bins, on the same Boson-sampling experiment are given by the $|bin_l^{(\text{sb})}\rangle$ configuration vectors, where

$$|bin_l^{(\text{sb})}\rangle = \bigcup_j |Y_j\rangle, \quad (2.28)$$

and the union over j can be chosen according to any agreed-upon strategy such that $1 \leq l \leq d^{(\text{sb})}$. In this paper, we consider the case where all bins contain an equal number of configuration vectors.

Given any binning strategy, the bin with the maximum probability is defined as $bin_{\text{true}}^{d^{(\text{sb})}}$, and the corresponding peak bin probability (PBP) is defined as μ_{true} . If the complete output bin probability distribution is unknown, the PBP μ_{net} of the incomplete probability distribution serves as an estimate of μ_{true} . That is, assuming that the honest nodes on the blockchain network provide enough samples for the same boson-sampling experiment, the PBP μ_{net} will be a close approximation to the PBP μ_{true} of the binned boson-sampling problem.

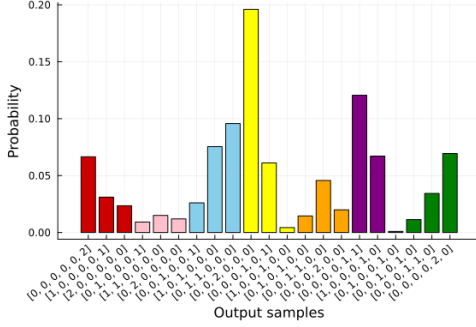
Specifically, we wish to ensure that,

$$\Pr[\mu_{\text{net}} - \epsilon/2 < \mu_{\text{true}} < \mu_{\text{net}} + \epsilon/2] > 1 - \gamma, \quad (2.29)$$

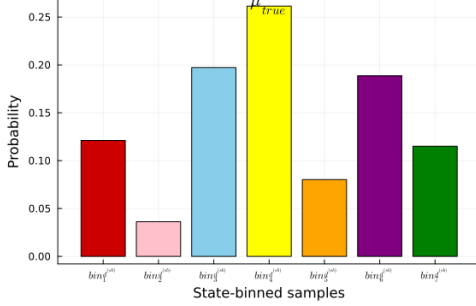
for some accuracy $\epsilon < 1/d^{(\text{sb})} \ll 1$ where $\gamma \ll 1$ determines the $100(1 - \gamma)\%$ confidence interval for μ_{true} . It was shown in Ref. [10] that this can be achieved for perfect boson sampling using a sample size of at least

$$N_{\text{tot}}^{(\text{sb})} = \frac{12d^{(\text{sb})}}{\epsilon^2} \ln(2\gamma^{-1}). \quad (2.30)$$

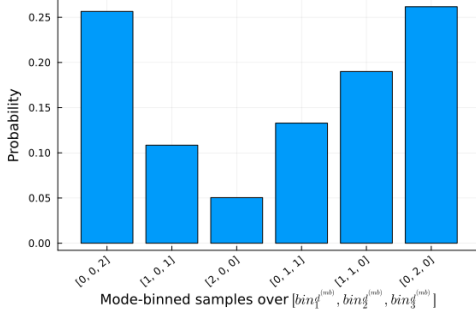
⁵ We ignore the cost to compute the $M \times M$ matrices $V(\mathbf{s})$ as this could be pre-computed for all \mathbf{s} since we assume a fixed unitary U in the protocol to follow.



(a) Boson-sampling probability distribution



(b) State-binned boson-sampling probability distribution



(c) Mode-binned boson-sampling probability distribution

Figure 3. Plots showing the output probability distribution of a Haar random boson-sampling device with two photons in six modes, i.e. $N = 2$ and $M = 6$, for which a total of $\binom{6+2-1}{2}$, i.e. 21 output photon configurations are possible. (a) BS distribution without any binning. The x-axis shows the different ways in which two photons can exit the six modes of the boson sampler and the corresponding probabilities of these configurations. (b) State-binned distribution of the same experiment where the 21-dimensional output Hilbert space is binned into $d^{(sb)} = 7$ bins, each bin containing three configurations chosen by the colour code as visible in both (a) and (b). Note that $\text{bin}_4^{(sb)}$ has the maximum probability of $\mu_{\text{true}} = 0.26$. (c) Mode-binned distribution of the same experiment where the modes are grouped into $d^{(mb)} = 3$ bins, each mode bin containing two consecutive bins. A total of $\binom{3+2-1}{2}$, i.e. 6 output photon configurations are possible for this mode-binning.

Using a bootstrap technique obtained by resampling provided samples from the boson-sampling distribution, it is shown [10] that the required accuracy can be obtained when $2d^{(sb)}\epsilon^{0.8} \lesssim 0.1$, in which case, if we demand a low uncertainty $\gamma = 10^{-4}$, the number of required samples is

$$N_{\text{tot}}^{(sb)} = 1.8 \times 10^5 d^{(sb)7/2}. \quad (2.31)$$

C. Variation of the protocol using Gaussian Boson-Sampling

While the original boson-sampling protocol described above is based on photon-number states, variants based on alternate types of input states have been described [24, 25]. Most notably, Gaussian boson-sampling [26], where inputs are squeezed vacuum states, has gained a lot of traction amongst experimental realisations owing to the relative ease and efficiency of preparing such states. Many of the protocols for photon generation were already making use of Gaussian states and post-selection, so the complexity of sampling from the output state when the input state is a Gaussian state was studied in detail [26]. Gaussian states can be characterised by their mean and variance. The simplest Gaussian states are coherent states. It is interesting to note that there is no quantum advantage in using coherent states as input states for boson sampling. In this variant of boson sampling, input states are taken to be squeezed vacuum states. The squeezing operator is given by,

$$\hat{S}(z) = \exp \left[\frac{1}{2}(z^* \hat{a}^2 - z \hat{a}^{\dagger 2}) \right], \quad z = r e^{i\theta}. \quad (2.32)$$

Let us assume a Gaussian Boson-Sampling setup with squeezed vacuum states in N of M modes and vacuum in the remaining $M - N$ modes. The initial state is,

$$|\psi_{\text{in}}\rangle = \prod_{j=1}^N \hat{S}_j(r_j)|0\rangle, \quad (2.33)$$

where r_j is the squeezing parameter for the j th mode, which is assumed to be real for simplicity. The symplectic transformation corresponding to the squeezing operations is

$$S = \begin{pmatrix} \oplus_{j=1}^M \cosh r_j & \oplus_{j=1}^M \sinh r_j \\ \oplus_{j=1}^M \sinh r_j & \oplus_{j=1}^M \cosh r_j \end{pmatrix}. \quad (2.34)$$

Then the covariance matrix for the output state after the input state passes through the interferometer described by U is

$$\sigma = \frac{1}{2} \begin{pmatrix} U & 0 \\ 0 & U^* \end{pmatrix} S S^\dagger \begin{pmatrix} U^\dagger & 0 \\ 0 & U^T \end{pmatrix}. \quad (2.35)$$

Now let the particular measurement record of photon number counts be $Y_k = (y_1^{(k)}, \dots, y_M^{(k)})$. Then the proba-

bility of finding that record is given by,

$$\Pr(Y_k) = |\sigma_Q|^{-1/2} |\text{Haf}(B_{Y_k})|^2, \quad \sigma_Q = \sigma + \frac{1}{2} \mathbb{I}_{2M}. \quad (2.36)$$

Here the matrix B_{Y_k} is a constructed from the matrix

$$B = U(\oplus_{j=1}^M \tanh r_j) U^T, \quad (2.37)$$

and is determined as follows. If $y_i = 0$ then rows and columns i of matrix B are deleted, otherwise the rows and columns are repeated y_i times. $\text{Haf}(\cdot)$ denotes the matrix Hafnian. Similar to the permanent, the Hafnian of a general matrix is also $\#P$ -hard to calculate. It has been shown that sampling from the output state is also hard in the case of Gaussian boson sampling.

We can think of analogous mode and state binned sampling for the Gaussian variant. For the mode-binned Gaussian boson sampling we will want to develop a validation scheme similar to the one described in [22]. Even though other methods exists for validating samples from Gaussian boson sampling [27], we would like to have a protocol similar to that was used for original boson-sampling. The detailed study of parameters involved including the required number of samples is beyond the scope of this paper.

The protocol is similar to Sec. II B 2. We start with the input state defined in Eq. 2.33. The squeezing parameter is taken so that the total average number of photons is close to $2N$. Then the probability, $P^{(\text{mb})}(\mathbf{n})$, of measuring the binned output configurations can be expressed as

$$P^{(\text{mb})}(\mathbf{n}) = \frac{1}{(N+1)^{d^{(\text{mb})}}} \sum_{\tilde{\mathbf{c}} \in \mathbb{Z}_{N+1}^{d^{(\text{mb})}}} \tilde{\chi} \left(\frac{2\pi \tilde{\mathbf{c}} \cdot \mathbf{n}}{N+1} \right) e^{-i \frac{2\pi \tilde{\mathbf{c}} \cdot \mathbf{n}}{N+1}}. \quad (2.38)$$

The calculation of the characteristic function is slightly different since now the input state does not have a fixed number of photons. It is as follows,

$$\chi(\mathbf{c}) = \sum_{n_k | k=1,2,\dots,m} P(\mathbf{n}) e^{i\mathbf{c} \cdot \mathbf{n}}. \quad (2.39)$$

It was shown in Ref. [28] (see Eq. 25 within reference) that the characteristic function for GBS is,

$$\chi(\mathbf{c}) = \frac{1}{\sqrt{\det(\mathbb{I} - Z(\mathbb{I} - \sigma_Q^{-1}))}}, \quad (2.40)$$

$$Z = \bigoplus_{k=1}^M \begin{bmatrix} e^{i \frac{2\pi c_k}{N+1}} & 0 \\ 0 & e^{i \frac{2\pi c_k}{N+1}} \end{bmatrix}. \quad (2.41)$$

Here σ_Q is related to the covariance matrix of the output state and is defined in Eq. 2.36, and $\tilde{\chi}(\tilde{\mathbf{c}})$ can be obtained from $\chi(\mathbf{c})$ by replacing all c_k 's in i^{th} bin to be

\tilde{c}_i (see Appendix B for more details). This function can now be used in Eq. 2.38 and evaluated at a polynomial number of points to obtain the exact binned distribution (see also Ref. [29] for an alternative approach using classical sampling of the positive P distribution to obtain an approximation of the mode binned distribution). The rest of the protocol is similar to that of Fock state boson-sampling.

III. A QUANTUM POW CONSENSUS PROTOCOL

We consider a PoW consensus with two types of binning, one used for validation to catch out cheaters, and one to reward miners. The former can be estimated with classical computers efficiently, while the latter does not have a known classical computation though it does have an efficient quantum estimation. Upon successful mining of a block, the output of both binning distributions will be added to the blockchain, meaning one part can be verified efficiently by classical computers while another part cannot. This will incentivize nodes using boson-sampling devices to verify prior blocks in the blockchain. The protocol is illustrated in Fig. 4 and a detailed description follows below. See Table C for a description of the various parameters.

1. A transaction, or bundle of transactions, is created on the network. All nodes are aware of the following set of input parameters:

$$\mathbf{Pm} = \{N, M, U, d^{(\text{mb})}, d^{(\text{sb})}, T_{\text{mine}}, \epsilon, \beta, R, P\}, \quad (3.1)$$

which is assumed to be constant over many blocks but can be varied to adjust the difficulty of the problem.

2. A new block b_j representing this transaction is created. It has a header $\text{header}(b_j)$ that contains summary information of the block including the parameter set \mathbf{Pm} , a hash derived from transactions in the block, a hash of the previous block header together with its validation record $\text{Rec}(b_{j-1})$ (discussed in step 7), and a timestamp.
3. The new block is sent to every node in the network. All nodes stake tokens to participate. Note this is different from a proof-of-stake protocol since here all miners stake the same amount of tokens and the probability of successfully mining a block is independent of the staked amount.
4. Miners implement boson-sampling [8] using devices like those illustrated in Figure 2, using N photons input into M modes ordered $\{1, 2, \dots, M\}$. A hash of the header is mapped to a permutation on the modes using a predetermined function a ,

$$a : H(\text{header}(b_j)) \rightarrow \Pi \in S_M. \quad (3.2)$$

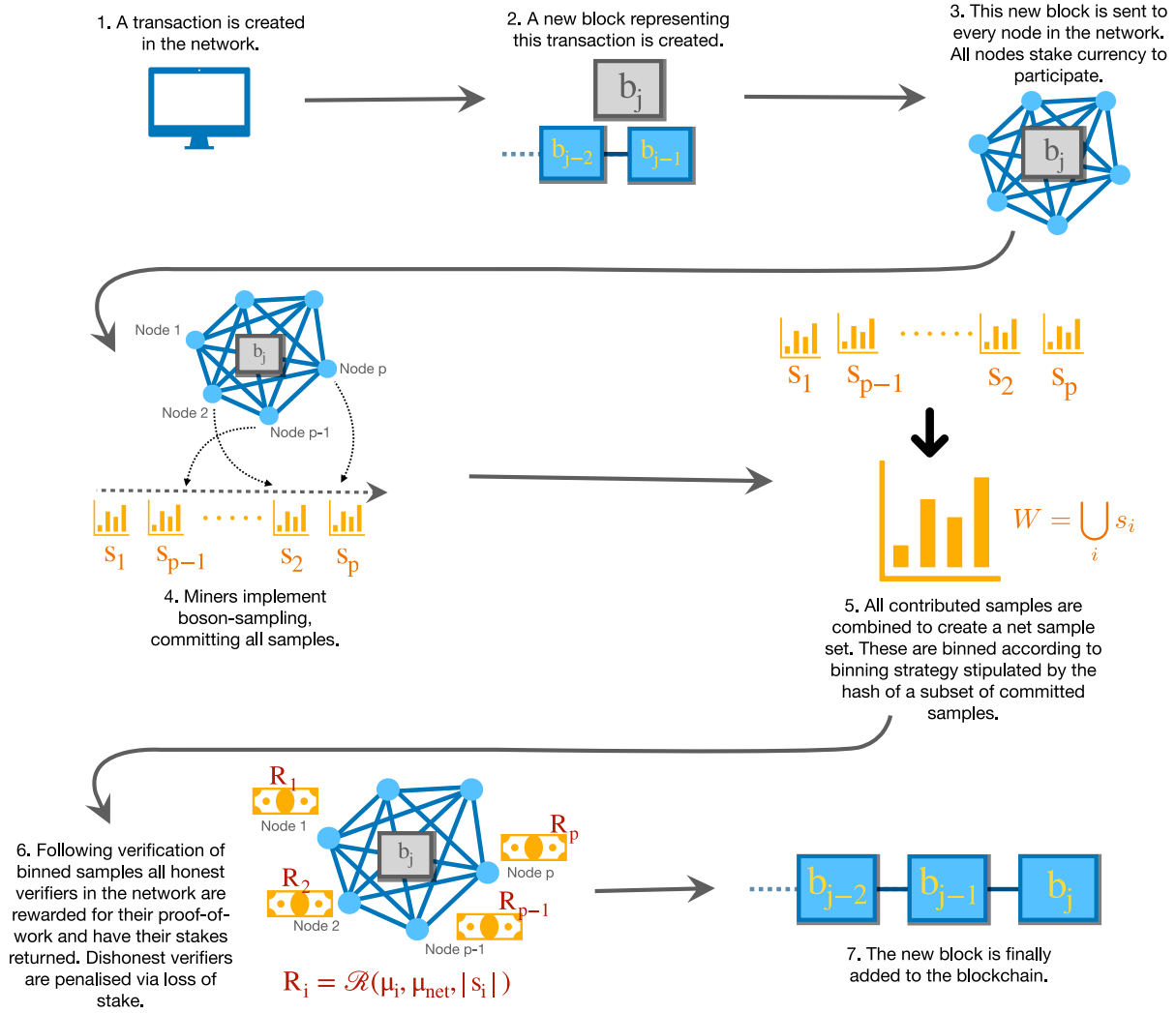


Figure 4. Blockchain architecture with the inclusion of boson-sampling routine.

This permutation, which depends on the current block, is used to determine the locations of the N input photons in the input state of the boson sampler. Each node i collects a set of samples denoted s_i , of size $|s_i|$, and commits each sample in the set by hashing that sample along with a timestamp and some private random bit string. The committed samples are broadcast to the network. The set of committed samples by node i is denoted \tilde{s}_i . The purpose of broadcasting hashed versions of the samples is to prevent dishonest miners from simply copying honest miners' samples.

5. After some predetermined mining time,

$$T_{\text{mine}} = \max\{N_{\text{tot}}^{(\text{mb})}, N_{\text{tot}}^{(\text{sb})}\}/R_q, \quad (3.3)$$

the mining is declared over and no new samples are accepted. All miners reveal their sample sets $\{s_i\}$ as well as the random bit strings associated with each sample so that the sets can be verified

against the committed sets $\{\tilde{s}_i\}$. If for some node i , the sets don't agree, that node is removed from further consideration of the mining round and they lose their stake. Let the set of remaining samples be $W = \bigcup_i s_i$.

6. This stage consists of three steps: a validation step using mode binning to catch dishonest miners, a state binning step to determine the mining success criterion and a reward/penalty payoff step.

- (a) *Validation.* A mode-binned distribution $P^{(\text{mb})}$ is used to validate each miner's sample set. Mode binning refers to grouping output modes into $d^{(\text{mb})}$ bins so that for a given sample the number of photon counts in a bin is simply the total number of ones at all the bit locations contained in the bin. We assume the bins are of equal size,

$$|\text{bin}_j^{(\text{mb})}| = M/d^{(\text{mb})} \quad \forall j. \quad (3.4)$$

A random beacon in the form of a string $\text{beacon}^{(\text{mb})}$ is announced to the network. Decentralized randomness beacons can be integrated into PoW consensus protocols in such a way that they are reliable, unpredictable, and verifiable. It would be advisable here to construct the beacons using post-quantum secure verifiable random functions [30, 31]. Using a predetermined function g ,

$$g : \text{beacon}^{(\text{mb})} \rightarrow \pi^{(\text{mb})} \in S_M, \quad (3.5)$$

the beacon is mapped to a permutation on the modes such that the modes contained in $\text{bin}_j^{(\text{mb})}$ are,

$$\{\pi^{(\text{mb})}(k)\}_{k=(j-1)M/d^{(\text{mb})}+1}^{jM/d^{(\text{mb})}}. \quad (3.6)$$

The mode-binned distribution for miner i is,

$$P^{(\text{mb})}[i] = \frac{1}{N|s_i|} (m_1[i], m_2[i], \dots, m_{d^{(\text{mb})}}[i]), \quad (3.7)$$

where $m_j[i]$ is the number of photon counts in $\text{bin}_j^{(\text{mb})}$ over the sample set s_i . The true mode binned distribution, $P^{(\text{mb})}$, that depends on $(\Pi, \pi^{(\text{mb})}, U)$, can be estimated as $\widehat{P}^{(\text{mb})}$ using a polynomial time classical algorithm. If the total variation distance between the distributions $\mathcal{D}^{(tv)}(\widehat{P}^{(\text{mb})}, P^{(\text{mb})}[i]) \geq 2\beta$ for some predetermined $0 < \beta < 1$ then the sample set s_i is invalidated and miner i loses their stake. Otherwise, the sample set is validated and labelled $s_i^{(v)}$. Let the set of validated samples be,

$$W^{(v)} = \bigcup_i s_i^{(v)}. \quad (3.8)$$

- (b) *Determining success criterion.* At this step a state binned distribution $P^{(\text{sb})}$ is computed to determine which miners are successful. First, it is necessary to sort the samples in $W^{(v)}$ into bins, a procedure referred to as state binning. The state space Y consists of $(N+1)$ ary valued strings of length M and weight N :

$$Y = \{Y_k\} = \{(y_1^{(k)}, \dots, y_M^{(k)})\};$$

$$y_j^{(k)} \in \mathbb{Z}_{N+1}, \sum_{j=1}^M y_j^{(k)} = N, \quad (3.9)$$

where the notation $y_i^{(k)}$ means for the k^{th} element of the sample space y_i photons were measured in the i^{th} mode. The states in Y are ordered lexicographically⁶. A second beacon $\text{beacon}^{(\text{sb})}$ is announced to the network

and using a predetermined function f ,

$$f : \text{beacon}^{(\text{sb})} \rightarrow \pi^{(\text{sb})} \in S_{|Y|}. \quad (3.10)$$

the beacon is mapped to a permutation on the state space. The states are sorted into $d^{(\text{sb})}$ equal sized bins such that the states contained in $\text{bin}_j^{(\text{sb})}$ are,

$$\{Y_{\pi(k)}\}_{k=(j-1)|Y|/d^{(\text{sb})}+1}^{j|Y|/d^{(\text{sb})}}. \quad (3.11)$$

All the publicly known samples in $W^{(v)}$ are then sorted into the bins and the collective state binned distribution is,

$$P^{(\text{sb})} = \frac{1}{|W^{(v)}|} (h_1, h_2, \dots, h_d), \quad (3.12)$$

where h_j is the number of samples in the $\text{bin}_j^{(\text{sb})}$. The PBP across the validated miners in the network is,

$$\mu_{\text{net}} = \frac{\max_j \{h_j\}}{|W^{(v)}|}. \quad (3.13)$$

Similarly, the PBP for validated miner i is,

$$\mu_i = \frac{\max_j \{|s_i^{(v)} \cap \text{bin}_j|\}}{|s_i^{(v)}|}. \quad (3.14)$$

- (c) *Payoff.* Miners whose samples were validated have their stake returned and are awarded a payoff if $|\mu_i - \mu_{\text{net}}| \leq \epsilon$ for some predetermined precision ϵ . The amount of the payoff is dependent on the number of samples committed.

7. The new block b_j is added to the blockchain with an appended record,

$$\text{Rec}(b_j) = \{\Pi, \pi^{(\text{mb})}, \pi^{(\text{sb})}, \widehat{P}^{(\text{mb})}, \mu_{\text{net}}\}. \quad (3.15)$$

This record contains the information necessary to validate the block.

IV. ANALYSIS OF THE PROTOCOL

A. Robustness

The key to making this protocol work is that the miners don't have enough information ahead of time about the problem to be solved to be able to pre-compute it but their samples can be validated after they have been committed. The blockchain is tamper-proof because any attempt to alter a transaction in a verified block of the chain will alter that block header and hence the input permutation Π that determines the boson-sampling problem and the output record **Rec**. One could also use a protocol where the unitary U depends on the block header

⁶ For example, for $M=3, N=2$ the ordering would be $\{(002), (011), (020), (101), (110), (200)\}$.

but it is easier to change the locations of input state photons than to reconfigure the interferometer circuit itself. The number of input states using N single photons in M modes is $\binom{M}{N}$ making precomputation infeasible.

The record $\text{Rec}(b_j)$ can be verified since the output distribution $P^{(\text{mb})}$ can be checked in polynomial time (in the number of bins $d^{(\text{mb})}$ and N) on a classical computer. The peak probability μ_{net} can be checked in polynomial time (in the number of bins $d^{(\text{sb})}$) on a quantum boson-sampler. The fact that the miners don't know the mode binning ahead of time, of which there are $M!/(M/d^{(\text{mb})})!d^{(\text{mb})}$ possibilities, means that even after the problem is specified, there is no advantage in using even classical supercomputers to estimate $P^{(\text{mb})}$. The probability of generating a random sample set that produces a correct mode-binned distribution within total variation distance β is no more than $\beta^{d^{(\text{sb})}-1}$, i.e. the probability to correctly guess to within β the probability in each bin (except the last which is given by normalization). Even if this probability were non-negligible, for example, because of a choice to use a small $d^{(\text{mb})}$ and large β to speed up the validation time, provided it is smaller than p^{cheat} , the protocol is robust. The reason is, as established in Sec. V, cheaters will be disincentivized since failure to pass the test incurs a penalty of lost staked tokens. Similarly, not knowing the state-binning means that they have no potential advantage in the payout.

The mining time is,

$$T_{\text{mine}} = \frac{\max\{N_{\text{tot}}^{(\text{mb})}, N_{\text{tot}}^{(\text{sb})}\}}{R_q}, \quad (4.1)$$

where R_q is based on publicly available knowledge of the boson sampling repetition rate at the time of the genesis block. This choice for mining time is made to ensure that honest miners with boson samplers will have produced enough samples to pass the validation test and even if there is only one honest node, that node will have produced enough samples to earn a reward. The repetition rate will of course increase with improvements in quantum technology but that can be accommodated for by varying the other parameters in the problem such as photon number, bin numbers, and prescribed accuracy, in order to maintain a stable block mining rate. For $N = 25$, $d^{(\text{mb})} = 3$, and $\beta = 0.1$, and assuming the boson sampling specs in Fig. 5, the minimum mining time would be 81.6s. The validation test sets a lower limit on the time to execute the entire protocol and add a new block. The classical computation involved during the validation step, while tractable, can be a long computation even for moderate sized bin numbers $d^{(\text{mb})}$ and photon numbers. Miners will be incentivized to use boson samplers to speed up this step of the consensus protocol.

The purpose of the state-binning step is twofold. It provides an independent way to tune the reward structure and hence moderate participation in the protocol. Second, it incentivizes nodes to have a quantum boson-sampling device in order to verify older blocks in the

blockchain since there is no known efficient classical simulation of the state-binned distribution whereas there is for the counterpart mode-binned distribution under the assumption of a constant number of bins.

B. Quantum vs. classical sampling rates

The time needed to successfully mine a block is determined by the inverse of the sampling(repetition) rate of the physical device. For a photonic boson sampler, the repetition rate is [32]

$$R_q = (\eta_f \eta_t^M)^N R_0 / N e. \quad (4.2)$$

Here R_0 is the single photon source rate and R_0/N is the rate at which N indistinguishable photons are produced, η_f is a parameter that doesn't scale with the number of modes and accounts for the preparation and detection efficiencies per photon. It can be written as the product $\eta_f = \eta_g \eta_c \eta_d$, where η_g is the photon generation efficiency, η_c is the coupling efficiency, and η_d is the detector efficiency. Finally, η_t is the beamsplitter transmission probability. Since we are assuming a circuit of depth equal to the number of modes (which is sufficient to produce an arbitrary linear optical transformation), the overall transmission probability per photon through the circuit is η_t^M . Finally, the factor of e is an approximation of the probability to obtain a collision-free event [33]. The experiment of Ref. [34] produced a single photon repetition rate of $R_0 = 76\text{MHz}$ and the experiment of Ref. [35], reported a transmission probability per photon through a 144×144 optical circuit of 97% implying a per beamsplitter transmission probability of $\eta_t = 0.97^{1/144}$ as well as an average wavepacket overlap of 99.5%. A value of $\eta_g = 0.84$ was reported for quantum dot sources in Ref. [36] and efficiencies of $\eta_c = 0.9843$ have been demonstrated for coupling single photons from a quantum dot into a photonic crystal waveguide [37]. Finally, single photon detector efficiencies of up to $\eta_d = 0.98$ have been reported at telecom wavelengths [38]. All these numbers can reasonably be expected to improve as technology advances [39].

The state-of-the-art general-purpose method to perform classical exact boson sampling uses a hierarchical sampling method due to Clifford & Clifford [40]. The complexity is essentially that of computing two exact matrix permanents providing for a repetition rate ⁷

$$R_c = \frac{1}{\tilde{a} \cdot 2 \cdot N \cdot 2^N}. \quad (4.3)$$

Here \tilde{a} refers to the scaling factor (in units of seconds s) in the time to perform the classical computation of the

⁷ We ignore the relatively small $O(MN^2)$ additive complexity to the classical scaling.

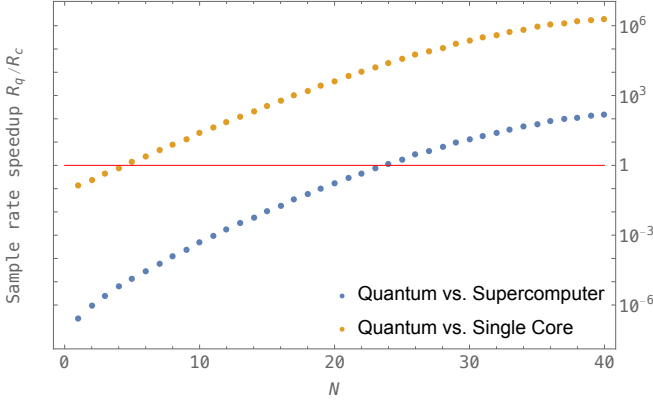


Figure 5. Sampling rate speed up R_q/R_c (log scale) for quantum boson-samplers relative to classical computers. Points above the red line indicate a quantum speedup. Orange dotted line: performance relative to single-core Intel Xeon processor running at 3.5GHz, and 128GB RAM with $\tilde{a} = 10^{-9.2}\text{s}$ [42]. Blue dotted line: performance relative to the Tianhe-2 supercomputer [43] with $\tilde{a} = N \times 1.99 \times 10^{-15}\text{s}^b$. The photonic boson-sampler is assumed to have the following specifications: single photon source rate $R_0 = 100\text{MHz}$, a single photon joint preparation and detection probability of $\eta_f = 0.90$, and beam-splitter transmission probability of $\eta_t = 0.9999$.

matrix permanent of one complex matrix where Glynn’s formula is used to exactly compute the permanent of a complex matrix in a number of steps $O(N2^N)$ using a Gray code ordering of bit strings. Recently an accelerated method for classical boson sampling has been found with an average case repetition rate scaling like $R_c = O(1.69^{-N}/N)$ [41], however, this assumes a linear scaling of the modes with the number of photons, whereas we assume a quadratic scaling.

As shown in Fig. 5 the performance ratio, defined as the ratio of sampling rates for quantum to classical machines R_q/R_c , is substantial even for a modest number of photons.

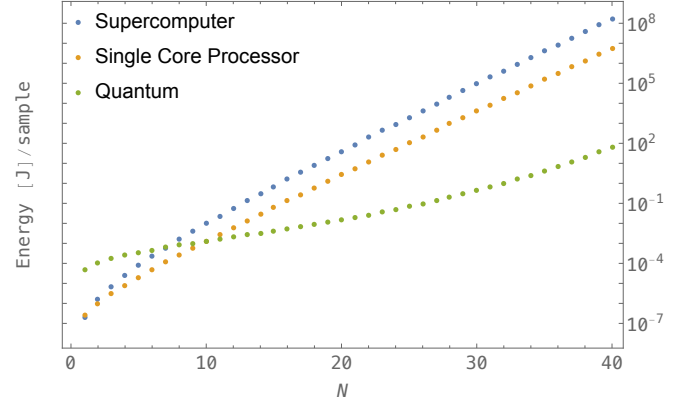


Figure 6. Comparison of the energy cost per sample (log scale) for boson-sampling using: a quantum boson-sampler, a supercomputer, and a single core processor all with same specs as in Fig. 5.

C. Quantum vs. classical energy cost

The energy cost to run boson samplers is dominated by the cost to cool the detectors since the cost to generate the photons and couple them into the device is negligible. Superconducting single-photon detectors of NbN type with reported efficiencies of $\eta_d = 0.95$ can operate at 2.1K [38] which is just below the superfluid transition temperature for Helium. Two-stage Gifford-McMahon cryocoolers can run continuously at a temperature of 2K with a power consumption of $\sim 1.5\text{kW}$ [38]. To compare the energy cost of boson-samplers to classical samplers, note that the power consumption of the Tianhe-2 supercomputer is 24MW [43], and the power consumption of a single core processor at 3.5GHz is $\sim 100\text{W}$. Ultimately, the important metric is the energy cost per sample since it is the accumulation of valid samples that enables a consensus to be reached. As seen from Fig. 6, quantum boson-samplers are significantly more energy efficient than classical computers. For example, at $N = 25$ photons the quantum boson-sampler costs $6.77 \times 10^{-2}\text{J}$ per sample which is 1563 times more energy efficient than a single core processor and 29569 times more efficient than a supercomputer.

While classical devices, such as ASICs, could be developed in the future that would speed up calculations of matrix permanents by some constant factor, any such device is fundamentally going to be limited by the exponential in N slowdown in the sampling rate (R_c in Eq. 4.3). Even as classical computers do speed up, one can increase the number of photons to maintain the same level of quantum advantage. Importantly, this would not require frequent upgrades on the boson sampler since the same device can accommodate a few more input photons as the number of modes was already assumed to be $O(N^2)$. Furthermore, as the quality of the physical components used for boson-sampling improves, the quantum

⁸ The extra factor of N comes from the fact that the parallelization here cannot directly implement Gray code ordering in the Balasubramanian–Bax–Franklin–Glynn algorithm (a variant of Ryser’s algorithm described in App. A). The quoted number is for the calculation done in 2018 using all available 16000 nodes on the supercomputer, each containing three CPUs and two co-processors.

repetition rates (R_q in Eq. 4.2) will increase, ultimately limited by the single photon source rate.

On the other hand, it is unlikely that much faster “quantum ASIC” devices will be developed for boson sampling. Fock state Boson sampling can be simulated fault tolerantly by universal quantum computers with polynomial overhead. One way to do this is to represent the state space as a truncated Fock space encoded in M qudits of local dimension $N + 1$ (or in $M \times \lceil \log(N + 1) \rceil$ qubits). The input state is a tensor product state of $|0\rangle$ and $|1\rangle$ states, the gates of the linear interferometer are two qudit gates which can be simulated in $O(N^4)$ elementary single and two qudit gates, and the measurement consists of local projectors such that the total simulation scales like $O(N^4 M^2)$. Another approach using the symmetric space of qudits is given in [44]. Given the algorithmic penalty as well as the gate overheads for error correction, the quantum computer based simulation would be slower than a photonic based native boson sampler, except in the limit of very large N where the fault tolerance of the former enables a speedup. However, at that point the entire protocol would be too slow to be of use for consensus anyway.

The improvements in the quantum repetition rates will hinge on advances in materials and processes that most likely would impose a negligible increase in energy cost. In this sense, PoW by boson sampling offers a route to reach a consensus without incentivizing users to purchase ever more power-hungry mining rigs.

V. PAYOFF MECHANISM

To reward nodes for their work done in the boson-sampling subroutine, nodes are rewarded when their individual PBP μ_i is sufficiently close to the net PBP μ_{net} . That is, a reward $R_i = \mathcal{R}(\mu_i, \mu_{\text{net}}, |s_i|)$ is paid to $node_i$ when $f(|\mu_i - \mu_{\text{net}}|) < \epsilon$ is satisfied. To prevent cheating, a penalty term $P_i = \mathcal{P}(\mu_i, \mu_{\text{net}}, |s_i|)$ is applied to $node_i$ when their individual PBP μ_i is far away compared to the net PBP μ_{net} (i.e. $f(|\mu_i - \mu_{\text{net}}|) \geq \epsilon$). The function f should be monotonic and we can assume it is linear in the argument.

We now construct a reward and penalty mechanism where it is the player’s unique dominant strategy to behave honestly in the boson-sampling subroutine and not cheat. We construct R_i and P_i so that it scales linearly with the number of samples provided by $node_i$. Denote this as $n \equiv |s_i|$. We also denote R to be the base rate reward for satisfying $f(|\mu_i - \mu_{\text{net}}|) < \epsilon$ with $n = 1$ and let P be the base rate penalty for satisfying $f(|\mu_i - \mu_{\text{net}}|) \geq \epsilon$ with $n = 1$. We also introduce a cutoff timestamp T_{mine} where only samples submitted prior to the cutoff time are considered for the payoffs. Finally, we denote the probability that an honest user satisfies the requirement $f(|\mu_i - \mu_{\text{net}}|) < \epsilon$ as p_i^{honest} and the probability that a cheater satisfies the requirement $f(|\mu_i - \mu_{\text{net}}|) < \epsilon$ as p_i^{cheat} .

This gives the expected reward and payoff for $node_i$ as,

$$\begin{aligned} \mathbb{E}[R_i] &= \begin{cases} np_i R & \text{if } t_i < T_{\text{mine}} \\ 0 & \text{otherwise} \end{cases}, \\ \mathbb{E}[P_i] &= \begin{cases} n(1 - p_i)P & \text{if } t_i < T_{\text{mine}} \\ 0 & \text{otherwise} \end{cases}, \end{aligned} \quad (5.1)$$

where p_i is either p_i^{honest} or p_i^{cheat} depending on the characteristics of $node_i$ as either a honest player or cheater. It is clearly sub-optimal to submit samples after the cut-off timestamp, thus the discussion going forward assumes that the player submits the samples prior to the cutoff time. There are 4 viable strategies for each player. They can:

- Submit an honest sample from a quantum boson sampler (denoted with an “honest” superscript)
- Exit the PoW scheme and submit nothing (denoted with a “nothing” superscript)
- Submit a cheating sample from any algorithm (denoted with a “cheat” superscript)
- Submit an honest sample from a classical algorithm (denoted with a “classical” superscript)

We now show that given some innocuous assumptions, a payoff mechanism can be constructed such that a unique pure strategy Nash equilibrium exists where each player’s dominant strategy is to submit an honest sample from a quantum boson sampler. To show this, we assume the following:

- A player’s utility is derived from the expected rewards minus the expected penalties and the costs incurred to generate a sample.
- An individual player’s sample contribution is significantly smaller than the combined sample of all players (i.e. $|s_i| \ll |s_{\text{total}}|$) so that μ_{net} remains unchanged irrespective of $node_i$ being honest or cheating.
- The verification subroutine is fairly accurate for $|s_i| \gg 1$ so that a honest player will satisfy $f(|\mu_i - \mu_{\text{net}}|) < \epsilon$ with probability $p_i^{\text{honest}} \in \mathbb{R}_{(0.75, 1)}$ and a cheater will satisfy $f(|\mu_i - \mu_{\text{net}}|) < \epsilon$ with probability $p_i^{\text{cheat}} \in \mathbb{R}_{(0, 0.25)}$.
- The cost to generate sample $\{s_i\}$ (denoted C_i) scales linearly with $|s_i|$. That is, $C_i = kn$, where $k \in \mathbb{R}$ and $n \equiv |s_i|$. The k parameter includes costs such as energy consumption to generate one sample but should not include sunk costs [45]. This assumption will be relaxed later to cover heterogeneous costs between players.
- The cost to generate a cheating sample is 0. This assumption will be relaxed later to cover cheating samples with costs.

We will cover the classical player later. Focusing on the first 3 strategies, the utilities are:

$$\begin{aligned}
u_i^{\text{honest}} &= \mathbb{E}[R_i] - C_i - \mathbb{E}[P_i] \\
&= np_i^{\text{honest}}R - nk - n(1 - p_i^{\text{honest}})P \\
&= n(p_i^{\text{honest}}R - k - (1 - p_i^{\text{honest}})P) \\
u_i^{\text{nothing}} &= 0 \\
u_i^{\text{cheat}} &= \mathbb{E}[R_i] - \mathbb{E}[P_i] \\
&= np_i^{\text{cheat}}R - n(1 - p_i^{\text{cheat}})P \\
&= n(p_i^{\text{cheat}}R - (1 - p_i^{\text{cheat}})P)
\end{aligned} \tag{5.2}$$

To ensure that the dominant strategy is for players to behave honestly and for cheaters to exit the scheme we require that

$$u_i^{\text{honest}} > u_i^{\text{nothing}} > u_i^{\text{cheat}}. \tag{5.3}$$

So we require,

$$\begin{aligned}
0 &< u_i^{\text{honest}} \\
\Rightarrow 0 &< p_i^{\text{honest}}R - k - (1 - p_i^{\text{honest}})P \\
0 &> u_i^{\text{cheat}} \\
\Rightarrow 0 &> p_i^{\text{cheat}}R - (1 - p_i^{\text{cheat}})P
\end{aligned} \tag{5.4}$$

Solving this, we obtain,

$$\frac{p_i^{\text{cheat}}R}{1 - p_i^{\text{cheat}}} < P < \frac{p_i^{\text{honest}}R - k}{1 - p_i^{\text{honest}}} \tag{5.5}$$

This inequality is not always defined. However, we note $p_i^{\text{cheat}} < p_i^{\text{honest}}$ and $\frac{1}{1-x}$ is increasing in $x \in \mathbb{R}_{(0,1)}$. So we have,

$$\frac{1}{1 - p_i^{\text{cheat}}} < \frac{1}{1 - p_i^{\text{honest}}}, \tag{5.6}$$

and a sufficient condition for inequality is,

$$\begin{aligned}
p_i^{\text{cheat}}R &< p_i^{\text{honest}}R - k \\
\Rightarrow \frac{k}{p_i^{\text{honest}} - p_i^{\text{cheat}}} &< R.
\end{aligned} \tag{5.7}$$

Since,

$$1 < \frac{1}{p_i^{\text{honest}} - p_i^{\text{cheat}}} < 2, \tag{5.8}$$

a sufficient condition for R is,

$$\frac{k}{p_i^{\text{honest}} - p_i^{\text{cheat}}} < 2k < R, \tag{5.9}$$

to ensure Eq. 5.5 is well-defined. Taking the tightest bounds for Eq. 5.5 and $2k < R$, we can bound P by,

$$\frac{1}{3}R < P < R. \tag{5.10}$$

These bounds ensure that,

$$u_i^{\text{honest}} > u_i^{\text{nothing}} > u_i^{\text{cheat}}, \tag{5.11}$$

is satisfied and the dominant strategy for $node_i$ is to be honest.

A. Classical Honest Players

To keep the PoW protocol quantum and to disincentivize classical players from submitting samples to the network would require the utility of classical players to be negative while keeping the utility of quantum players positive. From the construction above, we have already derived bounds for $node_i$ to be honest. We will keep these bounds and derive an upper bound for R that ensures $u_i^{\text{honest}} > 0$ and $u_i^{\text{classical}} < 0$.

We work under the assumption that the utility of a classical player is analogous to the utility of an honest player. That is,

$$u_i^{\text{classical}} = n(p_i^{\text{classical}}R - k^{\text{classical}} - (1 - p_i^{\text{classical}})P) \tag{5.12}$$

Where $p_i^{\text{classical}} = p_i^{\text{honest}}$ and $k^{\text{classical}} \gg k$. It is reasonable to think of a classical player as performing the boson-sampling subroutine using a classical simulator instead of a true quantum boson-sampler. Letting N be the number of photons and $M = N^2$ be the number of modes, the most efficient known classical boson-sampling simulator has a per sample cost proportional to the inverse of the repetition rate, R_c , defined in Eq. 4.3, i.e. $k^{\text{classical}} \in O(2^N N)$. In contrast, a quantum boson sampler has a per-sample cost proportional to the inverse of the repetition rate R_q (Eq. 4.2). In the ideal case ($\eta_f = \eta_t = 1$), this cost is linear in N , otherwise, it increases exponentially with N and M . However, as shown in Fig. 5 there is a large region of N values where this cost is several orders of magnitude smaller than that for classical supercomputers. Hence we can safely assume $k^{\text{classical}} \gg k$.

To have $u_i^{\text{classical}} < 0$, it is sufficient to have,

$$k^{\text{classical}} > R > p_i^{\text{classical}}R, \tag{5.13}$$

since $p_i^{\text{classical}} \in \mathbb{R}_{(0.75,1)}$. Combined with the derived bounds for $node_i$ to be honest, we have the bounds for R and P be,

$$2k < R < k^{\text{classical}}, \tag{5.14}$$

$$\frac{1}{3}R < P < R, \tag{5.15}$$

This ensures that $u_i^{\text{honest}} > 0$, $u_i^{\text{cheat}} < 0$, $u_i^{\text{classical}} < 0$, and $u_i^{\text{nothing}} = 0$ and the dominant strategy of $node_i$ is to submit an honest sample to the network using a quantum boson-sampler. This strategy is unique as strictly dominant Nash equilibria are unique [46].

B. Non-Nash Equilibrium without Penalty Term

[47] showed that under certain assumptions, deterministic tests to check PoW can have a Nash equilibrium that is in line with the consensus protocol's best interests. In this section, we show that contrary to deterministic tests to check PoW (such as running double SHA-256

in Bitcoin), a penalty term is a necessity for statistical tests that check PoW to ensure it is a Nash equilibrium for players to remain honest. This is because statistical tests imply a non-zero probability of passing the test even though a player may have submitted a cheating sample. A penalty term ensures that it is not optimal for the cheater to submit cheating samples in this manner.

Without a penalty term, the utilities of the players are:

$$\begin{aligned}
u_i^{\text{honest}} &= \mathbb{E}[R_i] - C_i \\
&= np_i^{\text{honest}} R - nk \\
&= n(p_i^{\text{honest}} R - k), \\
u_i^{\text{nothing}} &= 0 \\
u_i^{\text{cheat}} &= \mathbb{E}[R_i] \\
&= Np_i^{\text{cheat}} R,
\end{aligned} \tag{5.16}$$

where $n = |s_i^{\text{honest}}|$ is the number of samples committed by an honest player and $N = |s_i^{\text{cheat}}|$ is the number of samples committed by a cheater. To show that the honest strategy is not a Nash equilibrium, it suffices to show that $u_i^{\text{cheat}} > u_i^{\text{honest}}$. Let $N = \frac{np_i^{\text{honest}}}{p_i^{\text{cheat}}}$. Then,

$$\begin{aligned}
u_i^{\text{cheat}} &= Np_i^{\text{cheat}} R \\
&= \frac{np_i^{\text{honest}}}{p_i^{\text{cheat}}} p_i^{\text{cheat}} R \\
&= np_i^{\text{honest}} R \\
&> n(p_i^{\text{honest}} R - k) \\
&= u_i^{\text{honest}}.
\end{aligned} \tag{5.17}$$

In essence, when sample submission incurs negligible costs (i.e. $k = 0$) and without a penalty term, cheaters could artificially inflate their sample size in hopes of getting a large payoff by chance. This would result in a higher utility to act maliciously and destroy the original Nash equilibrium of being honest.

C. Heterogeneous Costs

We now relax the assumption that all players have the same cost factor k for generating one sample by a quantum boson-sampler and allow for a heterogeneous cost factor. That is, for player $i \in \{1, 2, \dots, p\}$ with cost function $C_i = k_i n$, $k_i \in \mathbb{R}_{>0}$ is potentially different along the players.

With heterogeneous costs, we set the cost factor k in Eq. 5.14 to the cost factor of the most efficient player (i.e. $k = \min\{k_1, k_2, \dots, k_p\}$). This ensures that there is at least one player (the most efficient player) such that,

$$u_{eff}^{\text{honest}} > u_{eff}^{\text{nothing}} > u_{eff}^{\text{cheat}}. \tag{5.18}$$

Since the sign of u_i^{cheat} is independent of the value of k , this also ensures that $u_i^{\text{cheat}} < u_i^{\text{nothing}} = 0$ for $i \in \{1, 2, \dots, p\}$. For inefficient players with individual cost

factors $k_i > k$ such that $u_i^{\text{honest}} < u_i^{\text{nothing}}$, the market mechanism will have the inefficient players leave the PoW scheme and submit nothing for verification.

If the variation in the individual cost factors is significant enough such that setting k to be the most efficient cost factor will result in the market becoming saturated, we can set k to be the m th lower percentile cost factor (i.e. $k = \min_{m\%}\{k_1, k_2, \dots, k_p\}$) so that we can ensure at least m per cent of the p players will have a positive payoff from contributing samples to the network and not exit the PoW scheme.

D. Cheating with Costs

If players have non-zero costs for generating a cheating sample, then it is clearly sub-optimal for players to cheat since cheating without costs is already a dominant strategy. Additional costs associated with cheating just make the utility for cheaters lower.

E. Block Reward vs. Split Reward

The derivations above assumed a split reward mechanism. That is, the reward for the addition of a new block is split between all players satisfying $f(|\mu_i - \mu_{\text{net}}|) < \epsilon$ and each player receives nR for their n samples provided. Another reward mechanism that could be used is a block reward mechanism in which the entire reward is awarded to one player instead of splitting it between players (i.e. one player satisfying $f(|\mu_i - \mu_{\text{net}}|) < \epsilon$ would randomly be chosen to receive the entire reward). While the expected reward would stay the same, there is now considerable variation in the payoff for the player. The initial assumption that the player's utility is risk-neutral and only depends on the expected rewards/penalties and costs would no longer be valid.

Conventional mean-variance utility theory in finance imposes a penalty term for risk-aversion due to the variability of the payoffs [48, 49]. Thus, for block reward mechanisms, it is more appropriate to use utility functions of the form

$$u_i = \mathbb{E}[R_i] - C_i - \mathbb{E}[P_i] - A_i \sigma^2. \tag{5.19}$$

Where A_i is the coefficient of risk-aversion for $node_i$ and σ^2 is the variance of the reward. It is difficult if not impossible to estimate the parameter A_i for all the players in the PoW protocol as it is intrinsically related to individual preferences of risk-aversion. We do not claim here that we can provide an estimate, empirical or theoretical, for its value. However, for implementation purposes, the reward R in Eq. 5.14 should be set higher for a block reward mechanism compared to a split reward mechanism so that the additional expected rewards $\mathbb{E}[R_i]$ would offset the penalty from risk-aversion $A_i \sigma^2$.

For implementation purposes of a block reward mechanism, it may also be prudent to consider safeguards

against selfish miners as proposed in [50]. In their paper, the authors discussed a mining protocol that deviated from the intended consensus protocol and had revenues scaling super-linearly against computational power once a threshold percentage of the network is dominated by one party (the authors upper bound this threshold by $1/3$). This is particularly relevant to block reward mechanisms due to the formation of mining pools to reduce the variance of payoffs. As such, it may be prudent to implement the solution proposed in [50] that raises the threshold to $1/4$. That is, whenever the blockchain forks and two branches of length one occur, instead of each node mining the branch that they received first, the protocol should dictate that they randomly and uniformly choose one of the two branches to mine. The act of this randomization safeguards against potential selfish miners that control less than $1/4$ of the computational power of the network.

F. Components of Costs (Variable k) and Cost to Entry

The cost variable k (or k_i for heterogeneous costs) is the amalgamation of all relevant costs to the generation of one sample. There is a distinction in this cost factor for players wishing to enter the boson-sampling scheme (prospective players) and for players already providing samples to the boson-sampling subroutine (current players).

For current players or players using a subscription-based cloud boson sampler, the cost factor k should only include the variable costs required to produce one sample to the sampling subroutine (e.g. subscription costs, electricity costs, boson preparation costs, measurement costs). That is, $k = k_{variable}$. The fixed cost of the boson-sampling device is sunk and its cost should not be taken into consideration for sampling decisions going forward [45].

For prospective players, however, the initial capital expenditure costs (e.g. source guides, detectors, machinery) must be taken into consideration for k . If τ is the expected number of samples the boson-sampler is expected to produce before obsolescence, then,

$$k = k_{variable} + \frac{k_{fixed}}{\tau}. \quad (5.20)$$

For the PoW protocol to be self-sustaining in the long run with consistent user renewal, the value for k in Eq. 5.14 must be above the k value for prospective players so that there are sufficient incentives for new players to overcome the cost to entry.

Two comments are worth adding here on the adoption of this new PoW consensus protocol. First, in the early stages, before large scale production and availability of boson samplers, it could be expected that classical miners would dominate. This could be accommodated for by having the reward inequality in Eq. 5.14 be initially

$R > k^{\text{classical}}$ so that the utility of classical players is positive. Then a decision could be made to gradually either (1) increase $k^{\text{classical}}$ (such as increasing the number of photons in the sampling problem and hence the difficulty) or (2) reduce R . This will kick classical players out of the protocol as they no longer have positive utility. Second, the conditions on reward and penalty described above assume that the Nash equilibrium is already reached since it is defined by the condition that no unilateral deviation will move the equilibrium. This will not be the case during the initialization stage of the protocol. During the genesis block and several blocks thereafter, additional mechanisms should be placed by trustworthy players, to ensure the initialization reaches this Nash equilibrium. The trustworthy players can then exit the market and the equilibrium will be retained, thus ensuring no “central authority” exists in the protocol.

VI. CONCLUSION

We have proposed a PoW consensus protocol that natively makes use of the quantum speedup afforded by boson-samplers. The method requires that miners perform full boson-sampling, where samples are post-processed as coarse-grained boson-sampling using a binning strategy only known after samples have been committed to the network. This allows efficient validation but resists pre-computation either classically or quantum mechanically. Whereas classical PoW schemes such as Bitcoin’s are notoriously energy inefficient, our boson-sampling-based PoW scheme offers a far more energy-efficient alternative when implemented on quantum hardware. The quantum advantage has a compounding effect: as more quantum miners enter the network the difficulty of the problem will be increased to maintain consistent block mining time, further incentivizing the participation of quantum miners.

The quantum hardware required for the implementation of our protocol has already been experimentally demonstrated at a sufficient scale and is becoming commercially available (Xanadu Borealis). While we have focused our analysis primarily on conventional Fock state boson-sampling, the method extends to Gaussian boson-sampling, accommodating faster quantum sampling rates owing to the relative ease with which the required squeezed vacuum input states can be prepared. We leave the detailed study of number of samples required, error tolerances, and performance of Gaussian boson-samplers to future work.

Like the inverse hashing problem in classical PoW, the boson-sampling problem has no intrinsic use. It would be interesting to consider if samples contributed to the network over many rounds could be used for some practical purpose, enabling ‘useful proof-of-work’, something that has also been suggested in the context of conventional blockchains [51].

ACKNOWLEDGEMENTS

We gratefully acknowledge discussions with Louis Tessler, Simon Devitt, and Peter Turner. GKB and GM received support from a BTQ-funded grant with

Macquarie University. GKB and PPR receive support from the Australian Research Council through the Centre of Excellence for Engineered Quantum Systems (project CE170100009). DS is supported by the Australian Research Council (ARC) through the Centre of Excellence for Quantum Computation and Communication Technology (project CE170100012).

-
- [1] C. Dwork and M. Naor, Pricing via processing or combatting junk mail, in *Advances in Cryptology — CRYPTO' 92*, edited by E. F. Brickell (Springer Berlin Heidelberg, Berlin, Heidelberg, 1993) pp. 139–147.
 - [2] L. K. Grover, A fast quantum mechanical algorithm for database search, in *Proceedings of the Twenty-Eighth Annual ACM Symposium on Theory of Computing*, STOC '96 (Association for Computing Machinery, New York, NY, USA, 1996) p. 212–219.
 - [3] T. Lee, M. Ray, and M. Santha, *Strategies for quantum races* (2018).
 - [4] S. Park and N. Spooner, *The superlinearity problem in post-quantum blockchains*, Cryptology ePrint Archive, Paper 2022/1423 (2022), <https://eprint.iacr.org/2022/1423>.
 - [5] P. W. Shor, Polynomial-time algorithms for prime factorization and discrete logarithms on a quantum computer, *SIAM Journal on Computing* **26**, 1484 (1997), <https://doi.org/10.1137/S0097539795293172>.
 - [6] D. Boneh and R. J. Lipton, Quantum cryptanalysis of hidden linear functions, in *Advances in Cryptology — CRYPTO' 95*, edited by D. Coppersmith (Springer Berlin Heidelberg, Berlin, Heidelberg, 1995) pp. 424–437.
 - [7] J. W. Z. Lau, K. H. Lim, H. Shrotriya, and L. C. Kwek, NISQ computing: where are we and where do we go?, *AAPPS Bulletin* **32**, 10.1007/s43673-022-00058-z (2022).
 - [8] S. Aaronson and A. Arkhipov, The computational complexity of linear optics, in *Proceedings of the Forty-Third Annual ACM Symposium on Theory of Computing*, STOC '11 (Association for Computing Machinery, New York, NY, USA, 2011) p. 333–342.
 - [9] G. M. Nikolopoulos and T. Brougham, Decision and function problems based on boson sampling, *Phys. Rev. A* **94**, 012315 (2016).
 - [10] G. M. Nikolopoulos, Cryptographic one-way function based on boson sampling, *Quantum Information Processing* **18**, 10.1007/s11128-019-2372-9 (2019).
 - [11] J. Dubrovsky, L. Kiffer, and B. Penkovsky, Towards optical proof of work, *Cryptoecon. Syst.* **11** (2020).
 - [12] S. Pai, T. Park, M. Ball, B. Penkovsky, M. Dubrovsky, N. Abebe, M. Milanizadeh, F. Morichetti, A. Melloni, S. Fan, O. Solgaard, and D. A. B. Miller, Experimental evaluation of digitally verifiable photonic computing for blockchain and cryptocurrency, *Optica* **10**, 552 (2023).
 - [13] A. Narayanan, J. Bonneau, E. Felten, A. Miller, and S. Goldfeder, *Bitcoin and Cryptocurrency Technologies: A Comprehensive Introduction* (Princeton University Press, USA, 2016).
 - [14] B. T. Gard, K. R. Motes, J. P. Olson, P. P. Rohde, and J. P. Dowling, From atomic to mesoscale (World Scientific, 2015) Chap. An introduction to boson-sampling, p. 167.
 - [15] J. Preskill, Quantum Computing in the NISQ era and beyond, *Quantum* **2**, 79 (2018).
 - [16] H.-S. Zhong, H. Wang, Y.-H. Deng, M.-C. Chen, L.-C. Peng, Y.-H. Luo, J. Qin, D. Wu, X. Ding, Y. Hu, P. Hu, X.-Y. Yang, W.-J. Zhang, H. Li, Y. Li, X. Jiang, L. Gan, G. Yang, L. You, Z. Wang, L. Li, N.-L. Liu, C.-Y. Lu, and J.-W. Pan, Quantum computational advantage using photons, *Science* **370**, 1460 (2020).
 - [17] L. S. Madsen, F. Laudenbach, M. F. Askarani, F. Rortais, T. Vincent, J. F. F. Bulmer, F. M. Miatto, L. Neuhaus, L. G. Helt, M. J. Collins, A. E. Lita, T. Gerrits, S. W. Nam, V. D. Vaidya, M. Menotti, I. Dhand, Z. Vernon, N. Quesada, and J. Lavoie, Quantum computational advantage with a programmable photonic processor, *Nature* **606**, 75 (2022).
 - [18] S. Arora and B. Barak, *Computational Complexity: A Modern Approach* (Cambridge University Press, 2009).
 - [19] M. Reck, A. Zeilinger, H. J. Bernstein, and P. Bertani, Experimental realization of any discrete unitary operator, *Physical Review Letters* **73**, 58 (1994).
 - [20] K. R. Motes, A. Gilchrist, J. P. Dowling, and P. P. Rohde, Scalable boson sampling with time-bin encoding using a loop-based architecture, *Phys. Rev. Lett.* **113**, 120501 (2014).
 - [21] L. Stockmeyer, The complexity of approximate counting, in *Proceedings of the Fifteenth Annual ACM Symposium on Theory of Computing*, STOC '83 (Association for Computing Machinery, New York, NY, USA, 1983) p. 118–126.
 - [22] B. Seron, L. Novo, A. Arkhipov, and N. J. Cerf, *Efficient validation of boson sampling from binned photon-number distributions* (2022).
 - [23] G. Valiant and P. Valiant, An automatic inequality prover and instance optimal identity testing, *SIAM Journal on Computing* **46**, 429 (2017), <https://doi.org/10.1137/151002526>.
 - [24] J. P. Olson, K. P. Seshadreesan, K. R. Motes, P. P. Rohde, and J. P. Dowling, Sampling arbitrary photon-added or photon-subtracted squeezed states is in the same complexity class as boson sampling, *Physical Review A* **91**, 022317 (2015).
 - [25] K. P. Seshadreesan, J. P. Olson, K. R. Motes, P. P. Rohde, and J. P. Dowling, Boson sampling with displaced single-photon fock states versus single-photon-added coherent states: The quantum-classical divide and computational-complexity transitions in linear optics, *Physical Review A* **91**, 022334 (2015).
 - [26] C. S. Hamilton, R. Kruse, L. Sansoni, S. Barkhofen, C. Silberhorn, and I. Jex, Gaussian boson sampling, *Physical Review Letters* **119**, 170501 (2017).
 - [27] A. S. Delliios, M. D. Reid, B. Opanchuk, and P. D. Drummond, Validation tests for gbs quantum computers us-

- ing grouped count probabilities (2022), [arXiv:2211.03480 \[quant-ph\]](#).
- [28] V. V. Kocharovsky, V. V. Kocharovsky, and S. V. Tarasov, The hafnian master theorem, *Linear Algebra and its Applications* **651**, 144 (2022).
- [29] P. D. Drummond, B. Opanchuk, A. Dellios, and M. D. Reid, Simulating complex networks in phase space: Gaussian boson sampling, *Phys. Rev. A* **105**, 012427 (2022).
- [30] Z. Li, T. G. Tan, P. Szalachowski, V. Sharma, and J. Zhou, Post-quantum vrf and its applications in future-proof blockchain system (2021), [arXiv:2109.02012 \[cs.CR\]](#).
- [31] M. Buser, R. Dowsley, M. F. Esgin, S. K. Kermanshahi, V. Kuchta, J. K. Liu, R. Phan, and Z. Zhang, Post-quantum verifiable random function from symmetric primitives in pos blockchain, Cryptology ePrint Archive, Paper 2021/302 (2021), <https://eprint.iacr.org/2021/302>.
- [32] C. Robens, I. Arrazola, W. Alt, D. Meschede, L. Lamata, E. Solano, and A. Alberti, Boson sampling with ultracold atoms (2022).
- [33] A. Arkhipov and G. Kuperberg, The bosonic birthday paradox, [arXiv 10.48550/ARXIV.1106.0849](#) (2011).
- [34] H. Wang, J. Qin, X. Ding, M.-C. Chen, S. Chen, X. You, Y.-M. He, X. Jiang, L. You, Z. Wang, C. Schneider, J. J. Renema, S. Höfling, C.-Y. Lu, and J.-W. Pan, Boson sampling with 20 input photons and a 60-mode interferometer in a 10^{14} -dimensional hilbert space, *Phys. Rev. Lett.* **123**, 250503 (2019).
- [35] Y.-H. Deng, Y.-C. Gu, H.-L. Liu, S.-Q. Gong, H. Su, Z.-J. Zhang, H.-Y. Tang, M.-H. Jia, J.-M. Xu, M.-C. Chen, H.-S. Zhong, J. Qin, H. Wang, L.-C. Peng, J. Yan, Y. Hu, J. Huang, H. Li, Y. Li, Y. Chen, X. Jiang, L. Gan, G. Yang, L. You, L. Li, N.-L. Liu, J. J. Renema, C.-Y. Lu, and J.-W. Pan, Gaussian boson sampling with pseudo-photon-number resolving detectors and quantum computational advantage (2023), [arXiv:2304.12240 \[quant-ph\]](#).
- [36] A. Zbiciak and T. Markiewicz, A new extraordinary means of appeal in the polish criminal procedure: the basic principles of a fair trial and a complaint against a cassatory judgment, Access to Justice in Eastern Europe **6**, 1 (2023).
- [37] M. Arcari, I. Söllner, A. Javadi, S. Lindskov Hansen, S. Mahmoodian, J. Liu, H. Thyrrestrup, E. H. Lee, J. D. Song, S. Stobbe, and P. Lodahl, Near-unity coupling efficiency of a quantum emitter to a photonic crystal waveguide, *Phys. Rev. Lett.* **113**, 093603 (2014).
- [38] L. You, Superconducting nanowire single-photon detectors for quantum information, *Nanophotonics* **9**, 2673 (2020).
- [39] Z.-E. Su, P. P. Rohde, J. Qin, C. Chen, M.-C. Chen, H.-S. Zhong, H. Wang, S. Höfling, C.-Y. Lu, and J.-W. Pan, Boson-sampling: from theory to post-classical computation (2023).
- [40] P. Clifford and R. Clifford, The classical complexity of boson sampling, in *Proceedings of the Twenty-Ninth Annual ACM-SIAM Symposium on Discrete Algorithms*, SODA '18 (Society for Industrial and Applied Mathematics, USA, 2018) p. 146–155.
- [41] P. Clifford and R. Clifford, Faster classical boson sampling (2020), [arXiv:2005.04214 \[quant-ph\]](#).
- [42] P. Lundow and K. Markström, Efficient computation of permanents, with applications to boson sampling and random matrices, *Journal of Computational Physics* **455**, 110990 (2022).
- [43] J. Wu, Y. Liu, B. Zhang, X. Jin, Y. Wang, H. Wang, and X. Yang, A benchmark test of boson sampling on Tianhe-2 supercomputer, *National Science Review* **5**, 715 (2018).
- [44] A. E. Moylett and P. S. Turner, Quantum simulation of partially distinguishable boson sampling, *Phys. Rev. A* **97**, 062329 (2018).
- [45] B. D. Bernheim and M. D. Whinston, *Microeconomics*, 2nd ed. (McGraw-Hill/Irwin, 2014).
- [46] S. Tadelis, *Game Theory: An Introduction*, 1st ed. (Princeton University Press, 2012).
- [47] J. A. Kroll, I. C. Davey, and E. W. Felten, The economics of bitcoin mining, or bitcoin in the presence of adversaries, The Twelfth Workshop on the Economics of Information Security (WEIS 2013) , 21 (2013).
- [48] H. Markowitz, Portfolio selection, *The Journal of Finance* **7**, 77 (1952).
- [49] R. E. Bailey, *The Economics of Financial Markets* (Cambridge University Press, 2005).
- [50] I. Eyal and E. G. Sirer, Majority is not enough: Bitcoin mining is vulnerable, *CoRR abs/1311.0243* (2013), [1311.0243](#).
- [51] A. Baldominos and Y. Saez, Coin.ai: A proof-of-useful-work scheme for blockchain-based distributed deep learning, *Entropy* **21**, 10.3390/e21080723 (2019).
- [52] Gurvits and Samorodnitsky, A Deterministic Algorithm for Approximating the Mixed Discriminant and Mixed Volume, and a Combinatorial Corollary, *Discrete & Computational Geometry* **27**, 531 (2002).
- [53] S. Aaronson and T. Hance, Generalizing and derandomizing gurvits's approximation algorithm for the permanent, *CoRR abs/1212.0025* (2012), [1212.0025](#).

Appendix A: Time complexity of estimation of matrix permanent using Gurvits algorithm

An additive approximation of the permanent of a matrix with complex entries was proposed by Gurvits [52, 53]. It follows by writing the permanent of a matrix $A \in \mathbb{C}^{n \times n}$ as the expectation value of a so-called Glynn estimator $Gly_{x_i}(A)$ over n bit random variables $x_i = (x_{i_1} x_{i_2} \dots x_{i_n})$ with $x_{ij} \in \{-1, 1\} \forall j \in [n]$:

$$\text{Per}(A) = E_{x_i \in \{-1, 1\}^n} [\text{Gly}_{x_i}(A)], \quad (\text{A1})$$

where,

$$\text{Gly}_{x_i}(A) = x_{i_1} x_{i_2} \dots x_{i_n} \prod_{j=1}^n (A_{j,1} x_{i_1} + \dots + A_{j,n} x_{i_n}). \quad (\text{A2})$$

Importantly, the Glynn estimator can be upper-bounded in its absolute values as follows:

$$|\text{Gly}_{x_i}(A)| \leq \|A\|^n, \quad (\text{A3})$$

where $\|A\|$ is the spectral norm of the A matrix, i.e. its largest singular value.

The algorithm to approximate the permanent of any such matrix A is then as follows:

1. Pick m number of n -bit strings: $x_1, x_2, \dots, x_m \in \{-1, 1\}^n$.
2. For each $i \in [m]$, compute $\text{Gly}_{x_i}(A)$. The average of these $\widehat{\text{Per}}(A) = \frac{1}{m} \sum_{i=1}^m \text{Gly}_{x_i}(A)$ is then the estimate of $\text{Per}(A)$.

Using Hoeffding's inequality, one can use the upper bound on $|\text{Gly}_{x_i}(A)|$ to write the following concentration bound for the mean of random Glynn estimators for some $\lambda > 0$:

$$\Pr(|\widehat{\text{Per}}(A) - \text{Per}(A)| \geq \lambda) \leq 2e^{-\frac{m\lambda^2}{2\|A\|^{2n}}}. \quad (\text{A4})$$

Setting $\lambda = \delta\|A\|^n$, one can then write,

$$\Pr(|\widehat{\text{Per}}(A) - \text{Per}(A)| < \delta\|A\|^n) \geq 1 - 2e^{-\frac{m\delta^2}{2}}. \quad (\text{A5})$$

Therefore, $m = O(1/\delta^2)$ samples suffice to approximate $\text{Per}(A)$ within $\pm\delta\|A\|^n$ additive error with high probability. Since for each random string $x_i \in \{-1, 1\}^n$, the Glynn estimator can be computed in $O(n^2)$ time, the complete algorithm for permanent approximation can be run in $O(n^2/\delta^2)$ time.

Moreover, if A is a unitary matrix or a sub-matrix thereof, $\|A\| \leq 1$. Hence each point in the characteristic function $\chi(\mathbf{s}) = \text{Per}(V_N(\mathbf{s}))$ can with probability at least p be computed to within additive error δ in time,

$$O\left(\frac{N^2 \ln(2/(1-p))}{\delta^2}\right). \quad (\text{A6})$$

Appendix B: Characteristic function for Gaussian Boson Sampling

In order to develop a validation protocol for Gaussian Boson Sampling similar to that for Fock state, we need to calculate the corresponding characteristic function. As before, the characteristic function is defined as,

$$\chi(\mathbf{c}) = \sum_{n_k | k=1,2,\dots,m} P(\mathbf{n}) e^{i\mathbf{c} \cdot \mathbf{n}}. \quad (\text{B1})$$

We have a closed form for this characteristic function that was calculated in Ref. [28] (see Eq. 25 within reference)

$$\chi(\mathbf{c}) = \frac{1}{\sqrt{\det(\mathbb{I} - Z(\mathbb{I} - \sigma_Q^{-1}))}} \quad (\text{B2})$$

$$Z = \bigoplus_{k=1}^M \begin{bmatrix} e^{ic_k} & 0 \\ 0 & e^{ic_k} \end{bmatrix} \quad (\text{B3})$$

Here σ_Q is related to the covariance matrix of the output state and is defined in Eq. 2.36.

The inverse Fourier transform to obtain $P(\mathbf{n})$ is as follows,

$$P(\mathbf{n}) = \int_{-\pi}^{\pi} \int_{-\pi}^{\pi} \cdots \int_{-\pi}^{\pi} \chi(\mathbf{c}) e^{-i\mathbf{c} \cdot \mathbf{n}} \prod_{j=1}^M \frac{dc_j}{2\pi}. \quad (\text{B4})$$

We would like to calculate the binned distribution $P^{(\text{mb})}(\tilde{\mathbf{n}})$ instead of $P(\mathbf{n})$.

$$P^{(\text{mb})}(\tilde{\mathbf{n}}) = \sum_{\mathbf{n} | \sum_{i \in \text{bin}_k} n_i = \tilde{n}_k} P(\mathbf{n}). \quad (\text{B5})$$

We can get this by manually introducing some delta functions in the inverse Fourier transform. We define $\tilde{\mathbf{c}}$, such that $\tilde{c}_k = c_i \forall i \in \text{bin}_k$.

$$\begin{aligned} & \int_{-\pi}^{\pi} \int_{-\pi}^{\pi} \cdots \int_{-\pi}^{\pi} \chi(\mathbf{c}) e^{-i\mathbf{c} \cdot \mathbf{n}} \prod_{k=1}^{d^{(\text{mb})}} \prod_{\{i,j\} \in \text{bin}_k} \delta(c_i - c_j) \prod_{j=1}^M \frac{dc_j}{2\pi} \\ &= \int_{-\pi}^{\pi} \cdots \int_{-\pi}^{\pi} \tilde{\chi}(\tilde{\mathbf{c}}) e^{-i\tilde{\mathbf{c}} \cdot \tilde{\mathbf{n}}} \prod_{k=1}^{d^{(\text{mb})}} \frac{d\tilde{c}_k}{2\pi} \end{aligned} \quad (\text{B6})$$

$$= \int_{-\pi}^{\pi} \cdots \int_{-\pi}^{\pi} \sum_{\mathbf{n}} P(\mathbf{n}) e^{i \sum_k \tilde{c}_k \sum_{j \in \text{bin}_k} n_j} e^{-i\tilde{\mathbf{c}} \cdot \tilde{\mathbf{n}}} \prod_{k=1}^{d^{(\text{mb})}} \frac{d\tilde{c}_k}{2\pi} \quad (\text{B7})$$

$$= \int_{-\pi}^{\pi} \cdots \int_{-\pi}^{\pi} \sum_{\mathbf{n}} P(\mathbf{n}) e^{-i \sum_k \tilde{c}_k (\tilde{n}_k - \sum_{j \in \text{bin}_k} n_j)} \prod_{k=1}^{d^{(\text{mb})}} \frac{d\tilde{c}_k}{2\pi} \quad (\text{B8})$$

$$\begin{aligned} &= \sum_{\mathbf{n}} P(\mathbf{n}) \underbrace{\int_{-\pi}^{\pi} \cdots \int_{-\pi}^{\pi} e^{-i \sum_k \tilde{c}_k (\tilde{n}_k - \sum_{j \in \text{bin}_k} n_j)} \prod_{k=1}^{d^{(\text{mb})}} \frac{d\tilde{c}_k}{2\pi}}_{= \prod_{k=1}^{d^{(\text{mb})}} \delta(\tilde{n}_k - \sum_{j \in \text{bin}_k} n_j)} \\ &= \sum_{\mathbf{n} | \sum_{j \in \text{bin}_k} n_j = \tilde{n}_k} P(\mathbf{n}) \end{aligned} \quad (\text{B9})$$

$$= \sum_{\mathbf{n} | \sum_{j \in \text{bin}_k} n_j = \tilde{n}_k} P(\mathbf{n}) \quad (\text{B10})$$

$$= P^{(\text{mb})}(\tilde{\mathbf{n}}) \quad (\text{B11})$$

Note in the second step above we have defined $\tilde{\chi}(\tilde{\mathbf{c}}) = \chi(\mathbf{c})$, where $c_i = \tilde{c}_k \forall i \in \text{bin}_k$. We can replace the integral with a summation over grid points since we are always restricted to a fixed photon number space, in which case we arrive at

$$P^{(\text{mb})}(\mathbf{n}) = \frac{1}{(N+1)^{d^{(\text{mb})}}} \sum_{\tilde{\mathbf{c}} \in \mathbb{Z}_{N+1}^{d^{(\text{mb})}}} \tilde{\chi}\left(\frac{2\pi\tilde{\mathbf{c}}}{N+1}\right) e^{-i\frac{2\pi\tilde{\mathbf{c}} \cdot \mathbf{n}}{N+1}}. \quad (\text{B12})$$

Appendix C: Parameters and description

	Notation	Description	Comments
BS setup	N	Total number of input photons	
	M	Total number of modes	We use $M = O(N^2)$
	U	Matrix description of linear optical circuit	$U \in \mathbb{C}^{M \times M}$
State-binned BS	$d^{(\text{sb})}$	Number of bins in the state Hilbert space	$d^{(\text{sb})} \lesssim 0.1/2\epsilon^{0.8}$
	μ_{true}	Peak bin probability (PBP) of state-binned BS	
	μ_{net}	Estimated PBP from all validated samples on the network	
	ϵ	Desired accuracy of the estimated PBP wrt. μ_{true}	
	$N_{\text{tot}}^{(\text{sb})}$	The number of samples needed across the network such that $ \mu_{\text{net}} - \mu_{\text{true}} \leq \epsilon$ with high confidence	$N_{\text{tot}}^{(\text{sb})} = 1.8 \times 10^5 d^{(\text{sb})7/2}$
	γ	$100(1 - \gamma)\%$ is the confidence interval for μ_{true}	We assume $\gamma = 10^{-4}$
Mode-binned BS	$d^{(\text{mb})}$	Number of bins in the mode Hilbert space	
	$P^{(\text{mb})}[i]$	Mode-binned probability distribution for miner i	
	m	Number of random samples needed to estimate matrix permanent up to an δ additive estimate with probability at least p , using Gurvit's algorithm	$m = \frac{2}{\delta^2} \ln(2/(1-p))$
	β	Accuracy parameter used to invalidate a miner's mode binned distribution based on total variation distance from an estimated mode binned distribution $P^{(\text{mb})}$ calculated using Gurvit's algorithm	$\mathcal{D}^{(\text{tv})}(\widehat{P^{(\text{mb})}}, P^{(\text{mb})}[i]) \geq 2\beta$
	$N_{\text{tot}}^{(\text{mb})}$	The number of samples sufficient for a quantum boson sampler to pass the validation test	$N_{\text{tot}}^{(\text{mb})} = 2^{16} \sqrt{\frac{(N+d^{(\text{mb})}-1)}{\beta^2}}$
	$m_j[i]$	Number of photons in the j^{th} bin for the i^{th} sample set s_i	
	$s_i^{(v)}$	Set of samples committed by the i^{th} node in the blockchain network.	The v superscript, if any, denotes the samples are validated
	$W^{(v)}$	The combined set of samples committed by all the nodes in the blockchain network	$W^{(v)} = \bigcup_i s_i^{(v)}$
Experimental resources	η_f	Combined parameter for single photon generation, coupling, and detection efficiency	
	η_t	Transmission probability of a single beam-splitter	
	R_0	Single photon repetition rate	
	R_q	Repetition rate of a quantum boson sampler	$R_q = (\eta_f \eta_t^M)^N R_0 / Ne$
Payoff mechanism	μ_i	Peak bin probability over the i^{th} verified sample set s_i^v	
	t_i	Time when the i^{th} user commits their samples to the network	
	p_i^{honest}	Probability of an honest user (either classical or quantum sampler) to pass the mode-binned BS test	
	p_i^{cheat}	Probability of a user providing non-BS samples to pass the mode-binned BS test	
	u_i^{honest}	Utility of an honest node in the network	
	u_i^{cheat}	Utility of a cheating node in the network	
	u_i^{nothing}	Utility of doing nothing, i.e. not committing any samples	
	$k^{\text{classical}}$	Cost per honest sample using classical algorithms	
	$k^{\text{quantum}} \equiv k$	Cost per honest sample using actual BS implementation	
	C_i	The cost incurred by the i^{th} node in committing $ s_i $ samples	
	P_i	Penalty implemented on the i^{th} node in the network	
	R_i	Reward awarded to the i^{th} node in the network	

Table I. List of parameters used in different modules of the algorithm.